2

DOE/MC/23270-2969
(DE91002055)

DOE/MC/23270--2969

DE91 002055

Task 1.0: Development of Improved Molten Carbonate Fuel Cell

Topical Report

W.H. Johnson

October 1990

Work Performed Under Contract No.: DE-AC21-87MC23270

For
U.S. Department of Energy
Office of Fossil Energy
Morgantown Energy Technology Center
Morgantown, West Virginia

MASTER

By
International Fuel Cells Corporation
South Windsor, Connecticut

DISTRIBUTION OF THIS DOCUMENT IS UNLIMITED

DISCLAIMER

This report was prepared as an account of work sponsored by an agency of the United States Government. Neither the United States Government nor any agency thereof, nor any of their employees makes any warranty, express of implied, or assumes any legal liability or responsibility for the accuracy, completeness or usefulness of any information, apparatus, product, or process disclosed, or represents that its use would not infringe privately owned rights. Reference herein to any specific commercial product, process, or service by trade name, trademark, manufacturer, or otherwise, does not necessarily constitute or imply its endorsement, recommendation, or favoring by the United States Government or any agency thereof. The views and opinions of authors expressed herein do not necessarily state or reflect those of the United States Government or any agency thereof.

This report has been reproduced directly from the best available copy.

Available to DOE and DOE contractors from the Office of Scientific and Technical Information, P.O. Box 62, Oak Ridge, TN 37831; prices available from (615)576-8401, FTS 626-8401.

Available to the public from the National Technical Information Service, U.S. Department of Commerce, 5285 Port Royal Rd., Springfield, VA 22161.

DOE/MC/23270-2969
(DE91002055)

Task 1.0: Development of Improved Molten Carbonate Fuel Cell

Topical Report

W.H. Johnson

Work Performed Under Contract No.: DE-AC21-87MC23270

For
U.S. Department of Energy
Office of Fossil Energy
Morgantown Energy Technology Center
P.O. Box 880
Morgantown, West Virginia 26507-0880

By
International Fuel Cells Corporation
P.O. Box 739
South Windsor, Connecticut 06074

October 1990

TABLE OF CONTENTS

	Page
INTRODUCTION	1
ABSTRACT	2
Subtask 1.3 – Design of Improved MCFC Cells	11
Subtask 1.4 – Development of Improved Matrices	18
Subtask 1.5 – Development of Anode-side Components	30
Subtask 1.6 – Development of Cathode-side Components	34
Subtask 1.7 – Development of End-Cell Reservoirs	37
Subtask 1.8 – Single Cell Testing of Improved Anode and Cathode Components Integrated into One Cell	38

LIST OF ILLUSTRATIONS

Figure		Page
1.3-1	Projection of Component Lithiation Consumption	13
1.3-2.	Time-to-Short Estimate	15
1.3-3.	Time-to-Short Estimate	16
1.4-1.	Accelerated Shorting Test (Cell No. 637)	23
1.4-2.	Strontium Electron Microprobe Results	26
1.4-3.	Effect of Current Density on Shorting Time	27
1.4-4.	Percent Seal Fill vs. Time	29
1.5-1.	Performance History of Cell No. 632	32
1.5-2.	Anode and Cathode Polarizations (Cell No. 653)	33
1.6-1.	Cell No. 660 Compaction Versus Time	36
1.8-1.	Anode and Cathode Polarizations (Cell No. 630)	39
1.8-2.	Performance History of Cell No. 639	40
1.8-3.	Performance History of Cell No. 647	41
1.8-4.	Performance History of Cell No. 655 (Third Integrated Cell)	42
1.8-5.	Performance History of Cell No. 663 (Fourth Integrated Cell)	43
1.8-6.	Performance History of Integrated Cell No. 673 (Seventh Integrated Cell)	44
1.8-7.	Performance of Cell No. 673 with Standard and Lean Oxidants	45
1.8-8.	Performance of Cell No. 673 with Standard and Lean Fuels	45
1.8-9.	Performance History of Cell No. 676 (Ninth Integrated Cell)	46

LIST OF TABLES

Table		Page
1	Cell Test and Performance Summary	4
1.3-1.	Projection of Component Lithiation Consumption	12
1.3-2.	Component Electrolyte Fill	13
1.4-1.	Cell Diagnostics (Cell No. 650)	19
1.4-2.	Cell Diagnostics	21
1.4-3.	Summary of Cell Shorting Data	24

INTRODUCTION

This report summarizes the work performed under Department of Energy Contract DE-AC21-87MC23270, "Molten Carbonate Fuel Cell Technology Improvement", on Task One. The work was separated into six technical subtasks.

Subtask 1.1, 1.2 – Program Management – provided the management function for this contract and the technical activities reported here.

Subtask 1.3 – Design of Improved MCFC Cells – defined improved cell designs directed toward meeting the performance, life, and cost goals of this contract. Two cell designs, one for the interior cells of a stack, and one for the cells at both ends of a stack, were conducted. Cell design requirements were established and used for generating the improved cell component designs. Preliminary designs for the anodes, cathodes, matrices, electrolyte reservoirs and reactant flow field distribution components were generated to guide the process development efforts in Subtasks 1.4 through 1.7. Feedback from these subtasks was assessed and integrated to modify the designs as required. Data from integrated single cell testing (Subtask 1.8) was used to establish the final design specifications for each cell component.

Subtasks 1.4 Through 1.7 – Development of Improved Matrices, Anode–Side Components, Cathode–Side Components, and End Cell Reservoirs – developed improved components for interior cells and end cells using new materials and configurations defined in the design subtask. These subtasks provided input to the design subtask in terms of component fabricability and scale-up, physical property measurements, and out-of-cell and single cell test results. The output of these subtasks was definition of scalable processes for fabricating components meeting design requirements and specifications.

Subtask 1.8 – Single Cell Testing of Improved Anode and Cathode Components Integrated into One Cell – evaluated the anodes, cathodes, and matrices developed in Subtasks 1.4 through 1.6 in integrated single cell tests. These tests determined cell component interactions and provided data for assessment in Subtask 1.3. Post-test analyses was conducted to verify that design requirements were met.

ABSTRACT

This report summarizes the work performed under Department of Energy Contract DE-AC21-87MC23270, Task One. The overall objective of this task was to develop an improved cell configuration for molten carbonate fuel cells which has improved performance, meets a 40,000 hour projected life, maintains existing cell cost, and is adaptable to a range of power plant applications.

A new cell configuration designed to be manufactured using conventional and available equipment and processes was developed and verified in subscale single cells. This means that manufacturing development is minimized and the potential for low cost is maximized.

This cell configuration is adaptable to a broad range of fuels without redesign. The same cell can operate on very weak low Btu coal gas as well as high Btu gas and natural gas.

The life of this cell configuration was extended significantly with the incorporation of end cell reservoirs, with reduced cell capacity and with the potential for an electrolyte change extending the time to short by almost a factor of two. Performance of the new cell configuration was improved by 55 mV/250 ASF.

The success of this technology program and the new cell configuration has provided the confidence to proceed with a scale-up to 8-ft^2 cells and a stack verification in a 20-cell, 25 kW stack test.

Design requirements and specifications for components in an improved cell design were defined. Electrolyte requirements for the cell components were established, the estimated time-to-short was updated, and a design operating point and gas composition for single cell testing was defined.

Four anode, four cathode, five matrix configurations, and three end-cell reservoirs were defined.

A total of fifty–four single cell tests were conducted to evaluate the performance of individual improvements and combinations of improved configurations. Tests were conducted at atmospheric pressure and 6.8 atmospheres.

Anodes were successfully fabricated by tape casting. Anodes with a smaller median pore size and broader pore size distribution showed better performance than a standard anode.

A new tape cast cathode for improved electrolyte sharing was developed. Single cell tests of cathode–side components show improved performance and lower compaction.

New tape cast matrix materials and matrix reinforcement were developed.

An end-cell reservoir configuration using conductive material was developed.

In a cell test with higher basicity electrolyte consisting of lithium carbonate–sodium carbonate, the time at which cell shorting occurred due to nickel oxide dissolution, was 80 percent greater than a standard cell.

Cell Test and Performance Summary

Single subscale cell tests were conducted to evaluate Molten Carbonate Fuel Cell improvements in the anode, the cathode, the matrix, end-cell reservoir and overall cell configurations.

Table 1 is a Cell Test and Performance Summary. This summary provides information on each cell test including the subtask under which the test was conducted, the start and end date of each test, the conditions of the test, purpose of the test, results, and the performance at both atmospheric pressure and 6.8 atmospheres.

Further details of each test are described in the sections for the specific subtask.

Table 1. Cell Test and Performance Summary

Cell No.	Sub-Task No.	Date Started	Date Terminated	Conditions of Test	Purpose of Test	Results	1 ATM 100 ASF (107 ma/cm^2) Peak Cell Volts (MV)[1]	1 ATM 100 ASF (107 ma/cm^2) Internal Resistance (MV)	6.8 ATM 160 ASF (172 ma/cm^2) Peak Cell Volts (MV)[2]	6.8 ATM 160 ASF (172 ma/cm^2) Internal Resistance (MV) at 100 ASF
624		12-18-87	1-11-88	A	Stand Checkout		790	56	-	-
625	1.4	1-7-88	3-11-88	A,P, S	Control cell for shorting test	Cell used for stand checkout	804	29	806	34
626		1-14-88	2-26-88	A	Determine electrode polarizations with ref. electrode	Ref. electrode data not valid	770	68	-	-
627	1.4	1-26-88	3-21-88	A, P, S	Control cell for shorting test	Shorted in 369 hours	806	39	827	39
628	1.4	2-2-88	3-31-88	A, P	Matrix Evaluation	Good	804	42	805	42
629	1.6	2-12-88	2-23-88	A	Measure performance of Config. A cathode	Performance poor.	781	47	-	-
630		2-22-88	4-4-88	A	Determine electrode polarizations with ref. electrode	Polarizations defined	800	43	-	-
632	1.5	2-25-88	7-22-88	A	Measure performance of Config. B anode	Performance good	800	46	-	-
633	1.4	3-4-88	4-7-88	A,P,S	Evaluate Config. A matrix in shorting test	Time to short reduced	831	29	821	30
634	1.6	3-9-88	4-14-88	A	Measure performance of Config. A cathode	Diffusional resistance present	800	52	-	-
635	1.6	3-15-88	4-19-88	A	Measure performance of Config. C cathode	Performance good	807	35-65	-	-

Table 1. Cell Test and Performance Summary (Cont'd)

Cell No.	Sub-Task No.	Date Started	Date Terminated	Conditions of Test	Purpose of Test	Results	1 ATM 100 ASF (107 ma/cm^2) Peak[1] Cell Volts (MV)	1 ATM 100 ASF (107 ma/cm^2) Internal Resistance (MV)	6.8 ATM 160 ASF (172 ma/cm^2) Peak[2] Cell Volts (MV)	6.8 ATM 160 ASF (172 ma/cm^2) Internal Resistance (MV) at 100 ASF
636	1.4	3-21-88	5-4-88	A, P, S	Evaluate effect of Config. B matrix on shorting	No effect on shorting time	815	43	829	29
637	1.4	3-31-88	4-29-88	A, P, S	Evaluate effect of $SrCO_3$ electrolyte on shorting	Time to short reduced	811	49	790	33
638	1.5	4-15-88	5-24-88	A	Measure performance of Config. C anode	Performance good	802	35		-
639	1.8	4-15-88	5-27-88	A	Integrated cell	Long time to reach peak performance	744	51	-	-
640	1.4	4-22-88	5-12-88	A, P	Evaluation effect of Li_2CO_3/Na_2CO_3 electrolyte on shorting	Test terminated due to seal leakage	< 821	25	< 840	24
641	1.6	5-3-88	6-7-88	A, P, S	Measure performance of Config. C cathode and shorting	Performance good	815	40	809	41
642	1.5	5-20-88	6-20-88	A	Measure performance of Config. D anode	Performance good	804	37	-	-
643	1.6	5-18-88	6-2-88	A	Measure performance of Config. C cathode with broader pore spectrum	Performance low	737	59	-	-

Table 1. Cell Test and Performance Summary (Cont'd)

Cell No.	Sub-Task No.	Date Started	Date Terminated	Conditions of Test	Purpose of Test	Results	1 ATM 100 ASF (107 ma/cm^2) Peak[1] Cell Volts (MV)	1 ATM 100 ASF (107 ma/cm^2) Internal Resistance (MV)	6.8 ATM 160 ASF (172 ma/cm^2) Peak[2] Cell Volts (MV)	6.8 ATM 160 ASF (172 ma/cm^2) Internal Resistance (MV) at 100 ASF
644	1.4	6-1-88	7-18-88	A, P, S	Evaluate effect of $SrCO_3$ electrolyte on shorting time	Time to short reduced	829	36	813	35
645	1.4	6-3-88	7-7-88	A, P, S	Evaluate effect of Li_2CO_3/Na_2CO_3 electrolyte and Config. C cathode on shorting	Time to short reduced	790	35	808	30
646	1.4	6-6-88	7-22-88	A, P, S	Evaluate effect of Li_2CO_3/Na_2CO_3 electrolyte on shorting	Shorted in expected time	827	25	826	24
647	1.8	6-14-88	7-13-88	A, P	Integrated cell	Performance good	814	37	807	34
648	1.6	6-22-88	7-12-88	A	Measure performance of Config. C cathode	Performance fair	794	61	-	-
649	1.5	7-6-88	10-4-88	A	Measure performance of Config. D anode (repeat of 642)	Anode performance good	795	52	-	-
650	1.4	7-12-88	8-17-88	A	Evaluate reinforced matrix	Performance good	835	34	-	-
651	1.6	7-24-88	10-26-88	A	Measure performance of Config. C cathode (repeat of cell 648)	Performance good	812	50	-	-
652	1.6	8-3-88	10-7-88	A	Measure performance of modified Config. B cathode	Performance high	824	50	-	-

Table 1. Cell Test and Performance Summary (Cont'd)

Cell No.	Sub-Task No.	Date Started	Date Terminated	Conditions of Test	Purpose of Test	Results	1 ATM 100 ASF (107 ma/cm^2) Peak[1] Cell Volts (MV)	1 ATM 100 ASF (107 ma/cm^2) Internal Resistance (MV)	6.8 ATM 160 ASF (172 ma/cm^2) Peak[2] Cell Volts (MV)	6.8 ATM 160 ASF (172 ma/cm^2) Internal Resistance (MV) at 100 ASF
653	1.5	8-9-88	11-9-88	A	Measure performance of Config. D anode with broad pore spectrum and reference electrode	Anode performance good Polarizations defined	800	53	–	–
654	1.6	8-12-88	9-27-88	A	Measure performance of alternative cathode structure	Performance low	678	78	–	–
655	1.8	8-24-88	9-30-88	A	Integrated cell	Performance fair	782	49	–	–
656	1.4	8-22-88	9-21-88	A,P,S	Evaluate effect of 250 ASF on shorting	Shorted in expected time	824	39	–	–
657	1.4	8-31-88	11-30-88	A,P,S	Evaluate effect of 0 ASF on shorting	Time to short extended	817	44	811	35
658	1.4	9-2-88	10-6-88	A,P,S	Evaluate effect of increased matrix thickness on shorting time	Time to short reduced	806	63	785	60
659	1.4	9-15-88	11-2-88	A,P,S	Evaluate effect of Li_2CO_3/Na_2CO_3 electrolyte on shorting	Time to short increased	807	32	770	57
660	1.6	10-5-88	11-2-88	A	Measure compaction of Config. C cathode	Low compaction	750	82	–	–
661	1.4	10-3-88	11-11-88	A,P,S	Effect of reinforced matrix on shorting time	Time to short not affected	817	46	821	46

Table 1. Cell Test and Performance Summary (Cont'd)

Cell No.	Sub-Task No.	Date Started	Date Terminated	Conditions of Test	Purpose of Test	Results	1 ATM 100 ASF (107 ma/cm^2) Peak[1] Cell Volts (MV)	1 ATM 100 ASF (107 ma/cm^2) Internal Resistance (MV)	6.8 ATM 160 ASF (172 ma/cm^2) Peak[2] Cell Volts (MV)	6.8 ATM 160 ASF (172 ma/cm^2) Internal Resistance (MV) at 100 ASF
662	1.4	10-11-88	4-13-89	A,P	Shorting time at less accelerated conditions	Shorted near expected time	836	44	842	33
663	1.8	10-19-88	11-23-88	A, P	Integrated cell	Performance good	803	80	770	76
664	1.5	10-24-88	1-18-89	A	Measure performance of modified Configuration D anode	Performance high	828	33	–	–
665	1.4	11-10-88	12-8-88	A	Evaluate alternative matrix strain distributor material	Build problem	790	33	–	–
666		12-1-88	12-8-88	A	Integrated cell	Build problem	622	185		
667		12-2-88	12-13-88	A	Effect of Config. B cathode on shorting time	Build problem	802	38		
668	1.4	12-6-88	1-12-89	A	Evaluate alternative $LiAlO_2$ matrix material	Performance high	827	36	–	–
669	1.4	12-7-88	3-10-89	A	Evaluate alternative matrix strain distributor material	Performance high	831	39	–	–
670	1.4	12-14-88	1-10-89	A,P,S	Effect of Cs_2CO_3 electrolyte additive on shorting time	Time to short reduced	828	36		
671	1.8	12-20-88	1-10-89	A	Integrated Cell	Initial performance fair, sudden performance loss	796	52		

Table 1. Cell Test and Performance Summary (Cont'd)

Cell No.	Sub-Task No.	Date Started	Date Terminated	Conditions of Test	Purpose of Test	Results	1 ATM 100 ASF (107 ma/cm^2) Peak[1] Cell Volts (MV)	1 ATM 100 ASF (107 ma/cm^2) Internal Resistance (MV)	6.8 ATM 160 ASF (172 ma/cm^2) Peak[2] Cell Volts (MV)	6.8 ATM 160 ASF (172 ma/cm^2) Internal Resistance (MV) at 100 ASF
672	1.4	1-13-88	4-17-89	A	Evaluate alternative matrix material, strain distributor	Performance high	847	25		
673	1.8	1-18-89	2-24-89	A,P	Integrated Cell	Performance good	818	48	826	40
674	1.8	1-25-89	2-16-89	A	Integrated Cell	Performance low	698	63		
675	1.4	1-25-89	3-7-89	A	Evaluate alternative matrix material, strain distributor, matrix reinforcement.	Performance high	845	25		
676	1.8	2-2-89	4-28-89	A,P	Integrated cell	Performance low	796	59	804	38
677	1.7	2-8-89	5-9-89	A,P	End cell reservoir	Performance low	700	66	682	45
680	1.8	2-22-89	2-28-89	A	Integrated cell	Shut down due to low performance	640	62		
689	1.8	5-3-89	5-8-89	A	Fill and start procedure	Performance low	729	60		
690	1.8	5-4-89	5-9-89	A	Fill and start procedure	Low open circuit voltage	758	106		

Table 1. Cell Test and Performance Summary (Cont'd)

Cell No.	Sub-Task No.	Date Started	Date Terminated	Conditions of Test	Purpose of Test	Results	1 ATM 100 ASF (107 ma/cm^2) Peak[1] Cell Volts (MV)	1 ATM 100 ASF (107 ma/cm^2) Internal Resistance (MV)	6.8 ATM 160 ASF (172 ma/cm^2) Peak[2] Cell Volts (MV)	6.8 ATM 160 ASF (172 ma/cm^2) Internal Resistance (MV) at 100 ASF
695	4.1	7-1-89	7-27-89	A,P	End cell reservoir	Performance good	792	38	815	37
699	4.1	8-23-89	Running	A,P	End cell reservoir (negative end)	Performance good	878	43	825	39

A – Ambient Conditions (1 ATM, 1200°F, GF-2, ROX-1**)*
P – Pressurized Conditions (6.8 ATM, 1200°F, GF-2, ROX-1)
S – Accelerated Testing Conditions (10 ATM, 1200°F, GF-2, 90% CO_2/10% O_2)

* *GF-2 Fuel contains 29.4% H_2, 5.5% CO, 17.5% CO_2, 47.5% H_2O*

** *ROX-1 Oxidant contains 8.7% O_2, 18.1% CO_2, 65.7% N_2, 7.4% H_2O*

1. Fuel: GF-2, H_2 + CO utilization 23% (57% at 250 ASF)
   Oxidant: ROX-1, CO_2 utilization 9% (25% at 250 ASF)
2. Fuel: GF-2, H_2 + CO utilization 36% (57% at 250 ASF)
   Oxidant: ROX-1, CO_2 utilization 16% (25% at 250 ASF)

SECTION 1

SUBTASK 1.3 - DESIGN OF IMPROVED MCFC CELLS

Objective

The objective was to design a cell configuration that meets the specific performance and life goals outlined below. The design activities included defining cell component requirements and specifications, supported by analytical studies and assessment of data generated in integrated cell tests, component cell tests, and out-of-cell tests.

- $\geq$ 0.717 volts at 250 amps-per-square foot performance using an oxygen-blown Texaco coal gasifier fuel at 85 percent utilization, operating at 100 psia.
- $\leq$ 4 mils of cell creep in 40,000 hours of projected stack life.
- Electrolyte management, independent of the reactant gas manifold seal properties, consistent with a 40,000-hour projected life for 8-ft^2 cells.
- Maintain existing cost associated with materials fabrication and assembly of cells and stack.
- Reactant flow distribution components that are readily adaptable to a broad range of power plant applications.

Design Operating Point and Gas Composition: An operating design point and the fuel and oxidant gas compositions for single cell testing were defined and are shown in Table 1.3-1.

The operating design point selected was 100 psia pressure, 1200°F and 250 ASF. These conditions were based on a systems optimization study conducted in the previous Department of Energy Molten Carbonate Development Program.

The fuel composition (see Table 1.3-1) represents the mixture produced by an oxygen-blown Texaco coal gasifier. This composition represents shift equilibrium at 1200°F. The oxidant composition contains 18.1 percent CO_2 which is selected to achieve the performance improvement goals of this program.

Electrolyte Requirements: A study was conducted to verify that the geometry of each of the components generated in the conceptual design was consistent with their electrolyte volume capacity and the required initial fill. Electrolyte loss due to lithiation of cell components was calculated for 40,000 hours of operation. The mechanisms of consumption included:

1. Lithiation of chrome in the anode-side components.
2. Lithiation of alumina in the matrix.
3. Lithiation of shee metal components.
4. Lithiation of nickel oxide in the cathode

Table 1.3-1. Design Operating Point and Gas Compositions

Pressure:	100 PSIA
Current Density:	250 ASF
Nominal Temperature	1200°F
ΔT	175°F
Voltage Per Cell:	0.717
Fuel Utilization:	85% (H_2 + CO)
Oxidant Utilization:	25% CO_2
Oxidant Composition (ROX-1)	
8.7% O_2	
18.1% CO_2	
65.7% N_2	
7.4% H_2O	
Fuel Composition (GF-2)	
29.4% H_2	
5.5% CO	
17.5% CO_2	
47.6% H_2O	

Other electrolyte loss mechanisms (creep and evaporation) were considered to be less significant and were not included.

Figure 1.3-1 shows the lithium carbonate consumption of the cell components as a function of time. The electrolyte inventory for each component is given in Table 1.3-2. For the assumed initial fills and the calculated lithiation losses, 22 percent of the available electrolyte is consumed. The results of this study indicated:

- The assumed interior cell configuration contains sufficient electrolyte inventory for 40,000 hours.
- The anode-side components operate in a satisfactory fill range of 28 - 50 percent.
- Testing is underway to verify whether cathode performance is satisfactory in the fill range. Pore size changes may be required if performance is not acceptable.

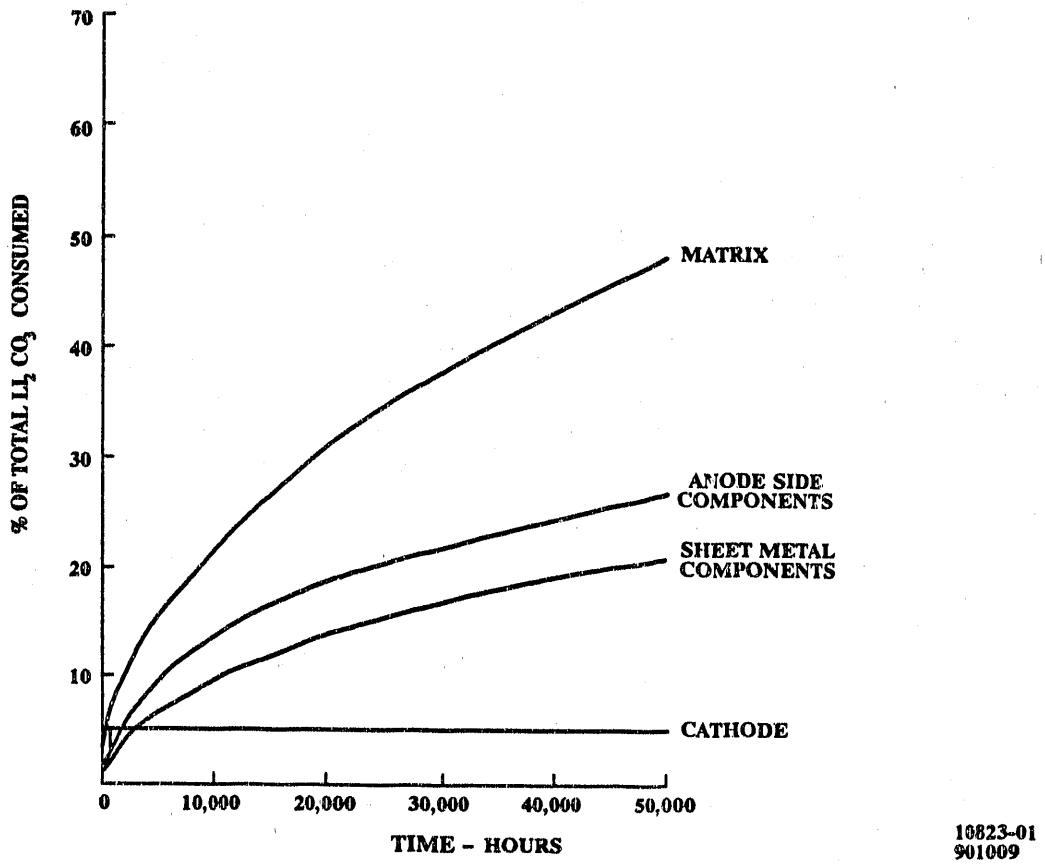

Figure 1.3-1. Projection of Component Lithiation Consumption

Table 1.3-2 Component Electrolye Fill

Component	Initial Percent Fill	40,000 Hours Percent Fill
Anode-side	50	28
Matrix	100	100
Cathode-side	65	51

Electrode Pore Size Requirements

Analyses were conducted to determine the pore size requirements for the anode and cathode to achieve improved electrolyte sharing. Single cell tests showed that the electrolyte fill of the cathodes in the new cell configurations is too high for optimum performance. Revised median pore sizes and broader pore size distributions are required for improved performance. The median pore sizes for the

anode and cathode were determined for three options to achieve improved electrolyte sharing. These included:

- Larger cathode median pore size, anode unchanged
- Smaller anode median pore size, cathode unchanged
- Combination of larger cathode and smaller anode median pore size.

These options provided the development effort in Subtasks 1.5 and 1.6 flexibility in the selection of materials and processes to meet the new requirements.

End-Cell Reservoir Requirements

Work was conducted to define the design requirements and specifications for end-cell reservoirs. Shunt current calculations defined the number of cells requiring reservoirs. The test data on the configuration to limit electrolyte transport out of the cell (Subtask 1.4) were studied to determine the effect on the end-cell reservoir design.

Electrolyte Transport to Manifold Seal

A shunt current analysis was conducted to evaluate the effect of resistance within the cell on electrolyte transport to the manifold seal. The table below shows that a very large resistance within the cell is required to reduce electrolyte transport to the manifold seal.

Relative Resistance Within Cell	Relative Total Electrolyte Transport Out of Cell
1.0	1.0
63	1.0
630	1.0
6300	0.36
∞	0

Data from the tests conducted in Subtask 1.4 showed electrolyte transport out-of-the-cell was reduced by 50 percent with a modified matrix configuration. However, to achieve essentially no electrolyte transport, the resistance within the cell must be increased by several orders of magnitude.

Matrix Shorting: The estimated time-to-short from NiO dissolution was updated. New information from additional literature sources was used. A comparison of the estimated and measured time-to-short for 30 single cell tests in the previous Department of Energy Molten Carbonate Development Program is shown in Figures 1.3-2 and 1.3-3. Figure 1.3-2 represents the updated estimate and Figure 1.3-3 was generated with the previous estimate. Comparison of the figures shows that a better correlation was obtained with the updated estimate. The updated estimate was used to define matrix design options that increase the time-to-short.

Preliminary Design Requirements and Specifications: A preliminary set of design requirements and specifications was prepared for each component in the cell configuration. The design requirements and specifications established for each cell component include the following:

Design Requirements:

- Component Overpotential and iR vs. Current Density
- Component Life
- Component Cost
- Component Compliance
- Component Creep Resistance

Design Specifications:

- Configuration
- Material
- Thickness and Area
- Porosity
- Mean Pore Size
- Pore Size Distribution
- Dimensional Tolerances
- Electrolyte Fill

Configuration Design: Preliminary drawings for candidate cell component configurations were prepared. The component configurations addressed include the following:

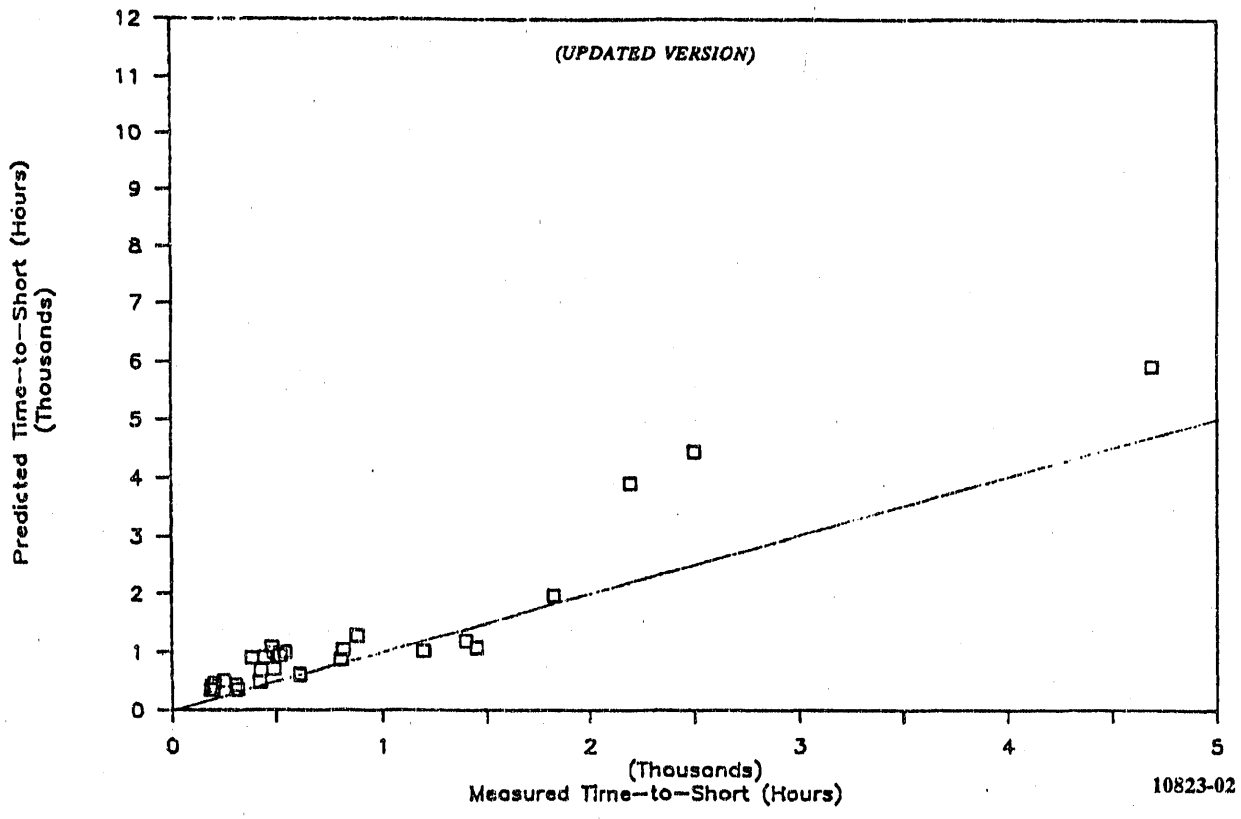

Figure 1.3-2. Time-to-Short Estimate

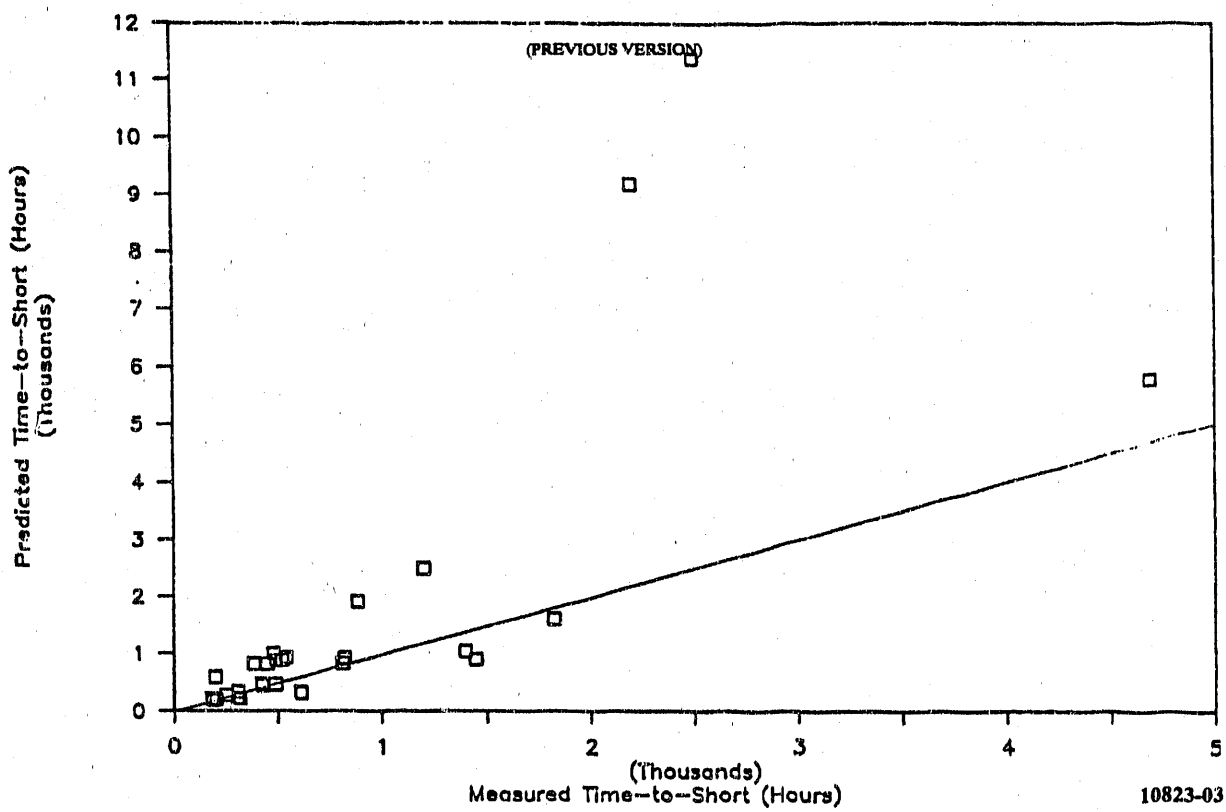

Figure 1.3-3. Time-to-Short Estimate

Anode Design

Four anode-side configurations were designed to reduce gas phase diffusional losses and to provide electrolyte storage capacity to meet a 40,000 hour life.

Cathode Design

Four cathode-side configurations were designed to reduce compaction, reduce NiO dissolution rates, and reduce gas phase diffusional losses.

Matrix Design

Three matrix configurations were designed to provide a higher tolerance to shorting caused by NiO dissolution products.

A matrix configuration that limits electrolyte transport out of the cell into the manifold seal was defined. Drawings were prepared to support out-of-cell component tests conducted in Subtask 1.4.

A matrix configuration that incorporates a reinforcement material and an alternative strain distributor material was defined.

End-Cell Reservoir Design

Three end-cell reservoir designs were defined. Two designs utilize a conductive reservoir material while the third design utilizes a non-conductive reservoir material. These designs were evaluated in single cell tests.

Based on the results of single cell tests Nos. 666 and 674, the end-cell reservoir design that utilizes a non-conductive reservoir material is considered unacceptable.

Also, one of the two end-cell designs that utilizes a conductive reservoir material has an unacceptable performance penalty based on testing of Cell No. 677.

The other end-cell design with a conductive reservoir material was evaluated in a single cell test with good performance verifying the approach.

The design specifications for the selected end-cell reservoir configuration were completed. This design utilizes a conductive reservoir material and is configured to have improved performance relative to the end-cell reservoir tested in Cell No. 677. Single cell tests (Nos. 695 and 699) conducted in Subtask 4.1 verified the improved performance.

Current Collector Design

The design of the stainless steel current collector was prepared to reduce gas-phase diffusional resistance.

The redesigned current collector was structurally analyzed using a finite element program. The results of this analysis showed stress levels to be acceptable. If the long term creep resistance of the present design is excessive, a 10 percent increase in material thickness would correct any deficiency.

Reactant Flow Fields Design

An analysis was conducted to determine the pressure drop for the anode and cathode flow fields for a power plant operating with an air-blown coal gasifier system. The pressure drops were determined to be acceptable using field heights of components used in the 8-ft^2 20-cell stack tested in the previous program.

Design for Manufacturability

Preliminary specifications and drawings were prepared for an alternative cell configuration designed for improved component manufacturability. This cell configuration consists of anode-side Configuration D and cathode-side Configuration D.

SUBTASK 1.4 - DEVELOPMENT OF IMPROVED MATRICES

Objective

Develop a matrix that increases cell performance by allowing the cathode to operate at higher CO_2 pressures. Identify matrix configurations that reduce electrolyte transfer from the matrix to the manifold seal, thereby allowing improved manifold sealability.

Matrix Process Development

The equipment required for tape casting subscale size matrices and seals was checked out and determined to be functionally acceptable. Trials were conducted to re-establish the tape matrix fabrication capability developed in the previous Department of Energy program.

Samples of several batches of lithium aluminate that were available from the previous program were submitted for physical property analyses including particle size distribution, surface area, particle shape, trace impurities, and crystalline structure. The lithium aluminate properties are important since they dictate the recipe of the slurry and the quality of the final matrix tape. Samples of new lithium aluminate were also submitted for physical property characterization.

The large batch from the previous program and the new batches were found to have acceptable properties. An order was placed for additional material for matrix and seal fabrication trials and single cell testing.

Subscale tapes were fabricated to provide the seal material required for single cell tests.

Matrices fabricated in the previous program for the 8-ft^2 short stack were used in the initial single cell tests that require a standard matrix. These matrices were either acceptable quality spares or parts with small defects that could be trimmed out. Samples of these matrices met shrinkage and porosity requirements. However, matrices fabricated in the previous program for the 8-ft^2 short stack were found to be unacceptable for use in single cell tests that require a standard matrix. Two cells (Nos. 624 and 626) which contained matrices fabricated in the previous program exhibited high iR, reactant gas crossover, and non-uniform wetting.

The tape matrix fabrication capability developed in the previous program was successfully re-established. Cell No. 628 was the first cell tested with a new tape matrix fabricated during this program. This cell had lower iR and higher open circuit than cells Nos. 624 and 626 as a result of the new tape matrix.

A matrix configuration was fabricated that is designed to concentrate the NiO dissolution products and increase the tolerance to shorting. Two cell tests (Nos. 625 and 627) were conducted to provide control data for the test of this matrix which was designed to concentrate NiO dissolution products. These cells were tested at high cathode carbon dioxide pressures to shorten the time at which shorting occurs. The results are discussed later.

A new supply of lithium aluminate powder was then procured. A complete analysis of the powder was completed including trace impurities, surface area, particle size distribution, particle shape and crystalline structure. The surface area of this lithium aluminate powder is higher than earlier supplies. Adjustments to the slurry were made to obtain acceptable tape cast matrices. This includes variations in the amounts of binder, surfactant, and dispersants. Porosity and pore size distribution were measured on trial parts to gauge acceptability.

Trials were conducted to incorporate a reinforcement material into the cell matrix to strengthen specific areas. Candidate materials and methods of incorporating the reinforcement into the matrix were evaluated. A material and process selection was made and matrices were fabricated for single cell testing. The first reinforced matrix was tested in Cell No. 650. Cell No. 650 was tested for 713 hours and was subjected to one crosspressure of 20 in. H_2O and three thermal cycles to 150°F. The cross cell leakage and open circuit potential change were measured periodically. There were no changes in these diagnostics as shown in Table 1.4-1, indicating acceptable matrix performance.

Table 1.4–1 Cell Diagnostics (Cell No. 650)

Load Time (Hrs)	Cross Cell Leakage (CCM at 5 in. water cross pressure)	Open Circuit Relative to Theoretical (mV)
177	13.5	0
	(Cell subjected to 20 in. H_2O cross pressure)	
321	5.0	0
	(Cell cooled to 150°F and reheated)	
338	4.0	0
	(Cell cooled to 150°F and reheated)	
480	9.0	0
594	8.0	0
	(Cell cooled to 150°F and reheated)	
617	10.0	0
711		0
713	Shut down	

Work was conducted to incorporate the new supply of lithium aluminate into tape cast matrices. Initial matrices fabricated with the new supply of lithium aluminate had acceptable median pore size, but higher porosity than obtained with earlier lithium aluminate supplies. Efforts to duplicate earlier matrix porosity by adjusting the slurry recipe did not result in reduced porosity. The higher porosity tape cast matrices were evaluated in single cell tests.

Matrices were then fabricated using an alternative strain distributor material. A single cell test (No. 665) was conducted to evaluate this matrix material change. The performance of Cell No. 665 was lower than expected (790 mV at 100 ASF and 1 ATM) due to high reactant leakage and cell crossover leakage. This is the result of a build error resulting in inadequate pinch on the cell. This cell was shutdown and the test repeated.

Cell No. 668 was tested to evaluate a matrix fabricated from the new supply of lithium aluminate. The performance of this cell was very good (827 mV at 100 ASF and 1 ATM). The initial open circuit voltage was lower than theoretical but the cell cross leakage was not unusually high (Table 1.4-2). After two shutdown cycles, both the open circuit voltage and cell cross over leakage were adversely affected. Inspection after shutdown showed some microcracking of the matrix but no gross indication of a problem.

Cell No. 669 (a repeat of Cell No. 655) was started to evaluate a matrix containing an alternative strain distributor material. The performance of Cell No. 669 was very good (831 mV at 100 ASF, 1 ATM). After 2132 hours of testing, which included three shutdown cycles, there was no significant change in open circuit voltage or cell cross leakage (Table 1.4-2).

Cell No. 672 was started to evaluate a matrix fabricated from a combination of the new lithium aluminate and strain distributor materials. Testing was completed after 2181 hours of load time. This cell had the highest performance to date (847 mV at 100 ASF and 1 ATM) and a low internal resistance (25 mV at 100 ASF). The cell diagnostics in Table 1.4-2 indicate good matrix integrity.

Cell No. 675 was started to evaluate the new matrix materials (lithium aluminate and strain distributor) in combination with matrix reinforcement. The performance of this cell was essentially the same as Cell No. 672. Peak performance measured 845 mV at 100 ASF, 1 ATM with an internal resistance of 25 mV at 100 ASF. The cell was subjected to two shutdown cycles. The low gas crossover leakage (Table 1.4-2) verifies the acceptability of this matrix configuration.

Table 1.4-2. Cell Diagnostics

Cell	Load Time (Hrs.)	Cell Cross Leakage (CCM at 5 in. H_2O Cross Pressure)	Open Circuit Relative to Theoretical (mV)
668	308	10	-14
		Cool Cell to 150°F and Reheat	
	325	33	-14
	637		-15
		Cool Cell to 150°F and Reheat	
	677	100	-24
	802	Shutdown	
669	155	--	0
		Cool Cell to 800°F and Reheat	
	189	0	0
	275		0
		Cool Cell to 150°F and Reheat	
	292	0	0
	604		0
		Cool Cell to 150°F and Reheat	
	645	8.0	0
	1228		0
	1820		0
	2095	0	
	2132		0
	2137	Shutdown	
672	136	--	0
	291	3.2	0
	760	--	0
	928	--	0
	1264		0
	1600		0
	1936		0
	2135	5.6	0
	2181	Shutdown	

Table 1.4-2. Cell Diagnostics (Continued)			
Cell	Load Time (Hrs.)	Cell Cross Leakage (CCM at 5 in. H_2O Cross Pressure)	Open Circuit Relative to Theoretical (mV)
672 (cont'd)	301	0	-6
		Cool Cell to 150°F and Reheat	
	316	5	-7
	580		-6
		Cool Cell to 150°F and Reheat	
	597	4	-10
	717		-11
	860		-10
	864	Shutdown	

Matrix Development to Improve Cell Performance

Matrix development was conducted on approaches to extend the time at which shorting occurs due to nickel oxide cathode dissolution. Two matrix variations were evaluated to reduce the effect of nickel oxide dissolution or the amount of dissolution. One approach is a matrix configuration that concentrates NiO dissolution products (Configuration A). This approach was expected to enable the matrix to hold more nickel before shorting occurs. Post test inspection of shorted cells tested previously showed nickel deposition in specific areas of the matrix. The matrix was altered to eliminate those areas (Configuration B).

The effect of increased electrolyte basicity on NiO dissolution was also evaluated.

The matrix and electrolyte changes were evaluated for their ability to extend the life before shorting occurs by testing the cells at conditions that accelerate the nickel oxide dissolution (90 m% CO_2, 10 m% O_2 at 10 atm. pressure).

The criterion for shorting was selected to be a drop of 10 mV in the cell open circuit voltage. Although the cells were operated on load, typically 160 ASF, during the shorting test, the open circuit voltage was monitored daily and a graph of open circuit voltage versus time was used to define the point when a 10 mV drop had occurred. A graph of open circuit history for Cell No. 637 is shown in Figure 1.4-1. The drop in open circuit voltage is verified to be caused by an electronic short by measuring the cell internal resistance during cell shutdown as the cell temperature drops below the solidification point of the electrolyte.

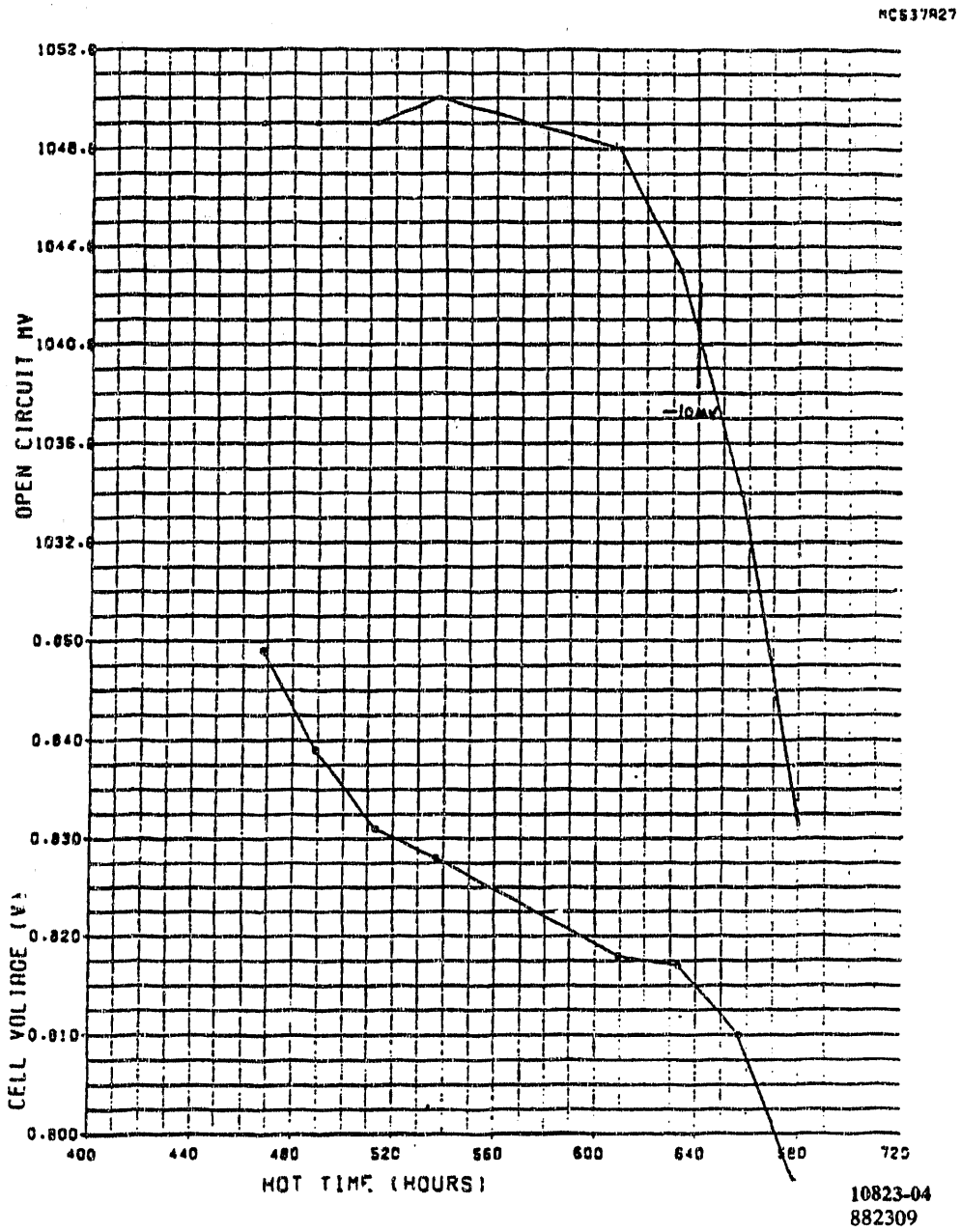

Figure 1.4-1. Accelerated Shorting Test (Cell No. 637)

Seventeen cells were tested to evaluate the matrix, electrolyte, and cathode changes. Fifteen of the cells completed accelerated shorting tests and two cells (Nos. 625 and 640) could not be subjected to accelerated tests due to operational problems. The results of the accelerated shorting tests are presented in Table 1.4-3.

Table 1.4-3. Summary of Cell Shorting Data

Cell No.	Description	Estimated Time-to-Short for Standard Cell (Hours)	Measured Time-to-Short (Hours)	Ratio Measured Estimated
627	Control Cell	297	369	1.24
633	Config. A Matrix	287	147	0.51
636	Config. B Matrix	255	310	1.22
637	$SrCO_3$ Added to Electrolyte	264	198	0.75
641	Li/K Electrolyte Config. C. Cathode	299	181	0.61
644	$SrCO_3$ Added to Electrolyte	424	304	0.72
645	Li/Na Electrolyte Config. C. Cathode	308	177	0.58
646	Li/Na Electrolyte	308	276	0.90
656	Effect of 250 ASF Operation	225	198	0.88
657	Effect of Open Circuit Operation	546	1558	2.85
658	Effect of Thicker Matrix	595	384	0.65
659	Li/Na Electrolyte	252	445	1.77
661	Reinforced Matrix	300	395	1.32
662	Control Cell	1676	> 1765	> 1.05
670	Cesium Carbonate added to Electrolyte	304	148	0.49

Two of the tests (Cells No. 625 and 627) were performed to provide control data for shorting tests. Cell No. 625 was used for stand checkout and was shut down prior to being put under accelerated conditions because an excessive cross pressure was imposed on the cell which would make the validity of the shorting data questionable. Cell No. 627 was tested at accelerated conditions until shorting occurred after 369 hours. This time is about the anticipated value for this cell at these conditions.

Cell No. 633 was tested to evaluate the Configuration A matrix designed to concentrate NiO dissolution products. This cell shorted in one-half the time of a standard cell, indicating the matrix change had an adverse effect.

Cell No. 636 was tested to evaluate the Configuration B matrix alteration to eliminate specific areas of nickel deposition. This cell shorted at a time about 20 percent longer than a standard cell. This longer time is within the predicted range for a standard cell, and therefore is not considered significant.

Cell No. 637 with strontium carbonate added to the lithium carbonate-potassium carbonate electrolyte to increase basicity shorted about 25 percent earlier than a standard cell. The performance of this cell was good as shown in Table 1. On an iR free basis, this cell had a performance of 0.860 volts at 100 ASF, the same as the best performing standard electrolyte cell (No. 633).

Another cell (No. 640) was tested to evaluate increased electrolyte basicity on shorting time. This cell had a lithium carbonate-sodium carbonate electrolyte. The initial performance and internal resistance were good (see Table 1), however, the accelerated shorting test could not be performed due to excessive seal leakage.

Cell No. 641 was tested to evaluate a Configuration C cathode. This cell shorted about 40 percent earlier than a standard cell.

Cell No. 644 was tested to evaluate an electrolyte with strontium carbonate added to the lithium carbonate-potassium carbonate electrolyte to increase basicity. This cell was similar in all respects to Cell No. 637 except that Cell No. 644 ran at 100 ASF versus 160 ASF for Cell No. 637. Cell No. 644 shorted about 30 percent earlier than a standard cell. This is about the same as Cell No. 637 which indicates no current density effect due to the presence of strontium carbonate. Both of these cell tests indicate the addition of strontium carbonate to the electrolyte has no beneficial effect in increasing the time at which shorting occurs. The cell performance is not adversely affected by the strontium carbonate as seen in Table 1. To determine why the strontium carbonate had no beneficial effect, Cell No. 637 was investigated after test by electron microprobe to determine the location of the strontium carbonate in the cell during operation. During cell shutdown, an attempt was made to maintain current flow through the cell as it was cooled to the electrolyte solidification temperature to minimize any redispersion of any strontium carbonate that might have segregated. The results shown in Figure 1.4-2 indicate that the strontium carbonate concentration was reduced in the cathode during cell operation, thereby reducing the effectiveness of the strontium carbonate in lowering the nickel oxide cathode solubility.

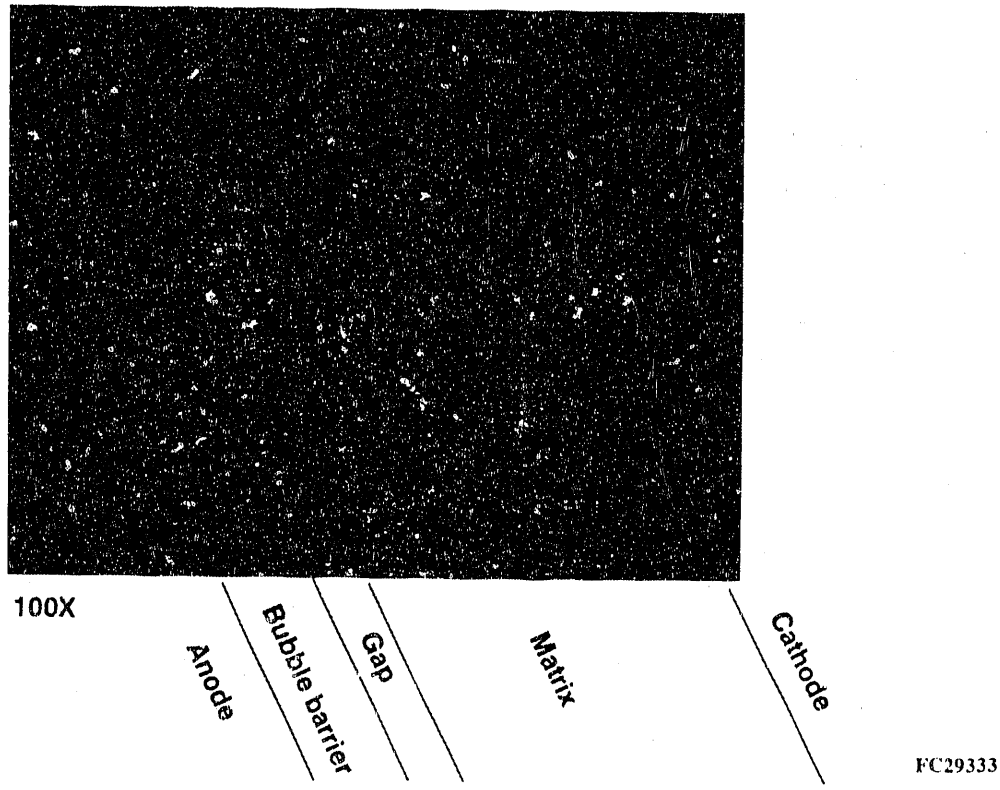

Figure 1.4-2. Strontium Electron Microprobe Results

Two cells (Nos. 645 and 646) were tested to evaluate a higher basicity electrolyte consisting of lithium carbonate-sodium carbonate. Cell No. 645 contained a Configuration C cathode and Cell No. 646 contained a standard cathode. Cell No. 645 shorted at a time 40 percent earlier than a standard cell and Cell No. 646 shorted at about the same time as a standard cell. These initial results indicated the lithium carbonate-sodium carbonate composition tested is not an improvement compared to the standard lithium carbonate-potassium carbonate electrolyte. Later tests on Cell No. 659 with this electrolyte discussed later showed an improvement in the time at which shorting occurs.

Two cells (Nos. 656 and 657) were tested to investigate the effect of current density on the time at which shorting occurs. Cell No. 656 was tested at 250 ASF and followed the predicted trend since it shorted at about 90 percent of the estimated time. Cell No. 657 was tested at open circuit. This cell did not follow the predicted trend since the time before shorting was about three times greater than the estimated time. A comparison of the predicted effect of current density with these cells and those containing the strontium carbonate additive is shown in Figure 1.4-3.

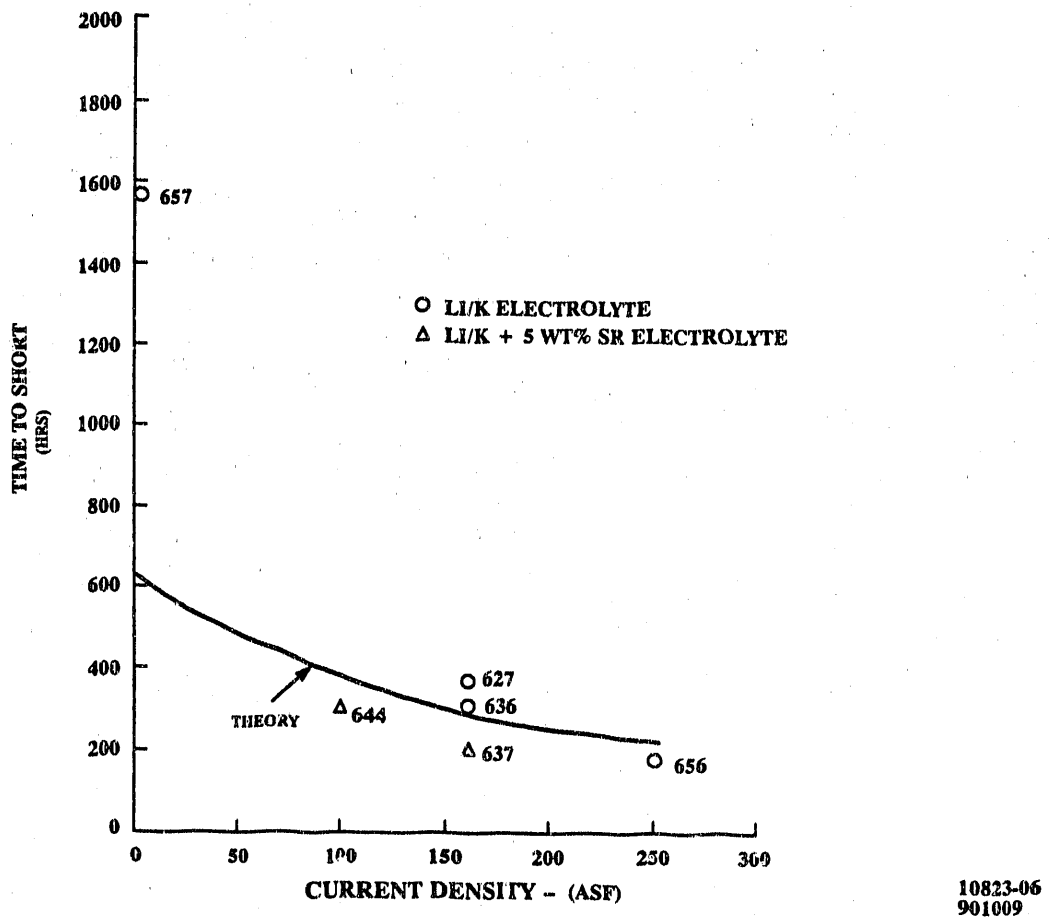

Figure 1.4-3. Effect of Current Density on Shorting Time

Cell No. 658 was tested to evaluate the effect of increasing matrix thickness. The matrix thickness in this cell was about twice the standard thickness. The measured shorting time was only 65 percent of the estimated shorting time. Post-test measurements showed this cell had a higher cell resistance than other cells which had shorted. Although shorting had begun, it may not have progressed to the level of other shorted cells.

Cell No. 659 was tested to evaluate a higher basicity electrolyte consisting of lithium carbonate-sodium carbonate. This cell shorted at a time about 80 percent greater than a standard cell, indicating the electrolyte composition tested represents an improvement over the standard lithium carbonate-potassium carbonate composition.

Cell No. 661 was subjected to an accelerated shorting test to evaluate a reinforced matrix. This cell shorted at a time about 30 percent longer than a standard cell indicating no adverse effect from the matrix reinforcement.

Cell No. 662 is a standard configuration cell that was tested to determine the shorting time at less accelerated conditions than normally used. The cell was operated at 250 ASF, 6.8 ATM, GF-2 fuel, and ROX-1 oxidant.

Cell No. 670 evaluated the effect of adding cesium carbonate to the electrolyte. This cell shorted at 49 percent of the expected time indicating that cesium carbonate addition was not effective.

Matrix Development to Reduce Electrolyte Transfer

A matrix configuration that is designed to limit electrolyte transport out of the cell into the manifold seal was defined. An out-of-cell test rig was designed and fabricated to evaluate this matrix configuration. The rig simulates the corners of a stack including the reactant manifold seals. It includes four repeat cell units with eight edges available for the cells to contact the manifold seals. Each test incorporates the modified matrix design in half of each cell and the standard matrix design in the other half of each cell to serve as a control for comparing electrolyte transfer into the manifold seal.

Matrices were fabricated for a series of tests. The first test was intended primarily for rig checkout. The results of this test identified some deficiencies in the design and operation of the rig. These deficiencies were corrected and a test of 100 hours duration was conducted. Results showed that the modified matrix configuration allowed approximately 50 percent of the electrolyte from the internal components to reach the simulated manifold seal compared to the standard matrix configuration.

The rig was reassembled and a 200 hour test was conducted. The data closely followed the initial 100 hour test with about one-half of the electrolyte reaching the simulated manifold seals with the modified matrix configuration as compared with the standard matrix configuration. The results of the tests are shown in Figure 1.4-4.

The results indicate that the matrix configuration tested does not reduce the amount of electrolyte transport to the manifold seal to an acceptable level. A shunt current analysis indicated the resistance within the cell must be increased by several orders of magnitude to sufficiently reduce electrolyte transport. Based on these results, future effort will be focused on developing a manifold seal with increased resistance to electrolyte transport. The manifold seal activity is reported in Subtask 4.1.

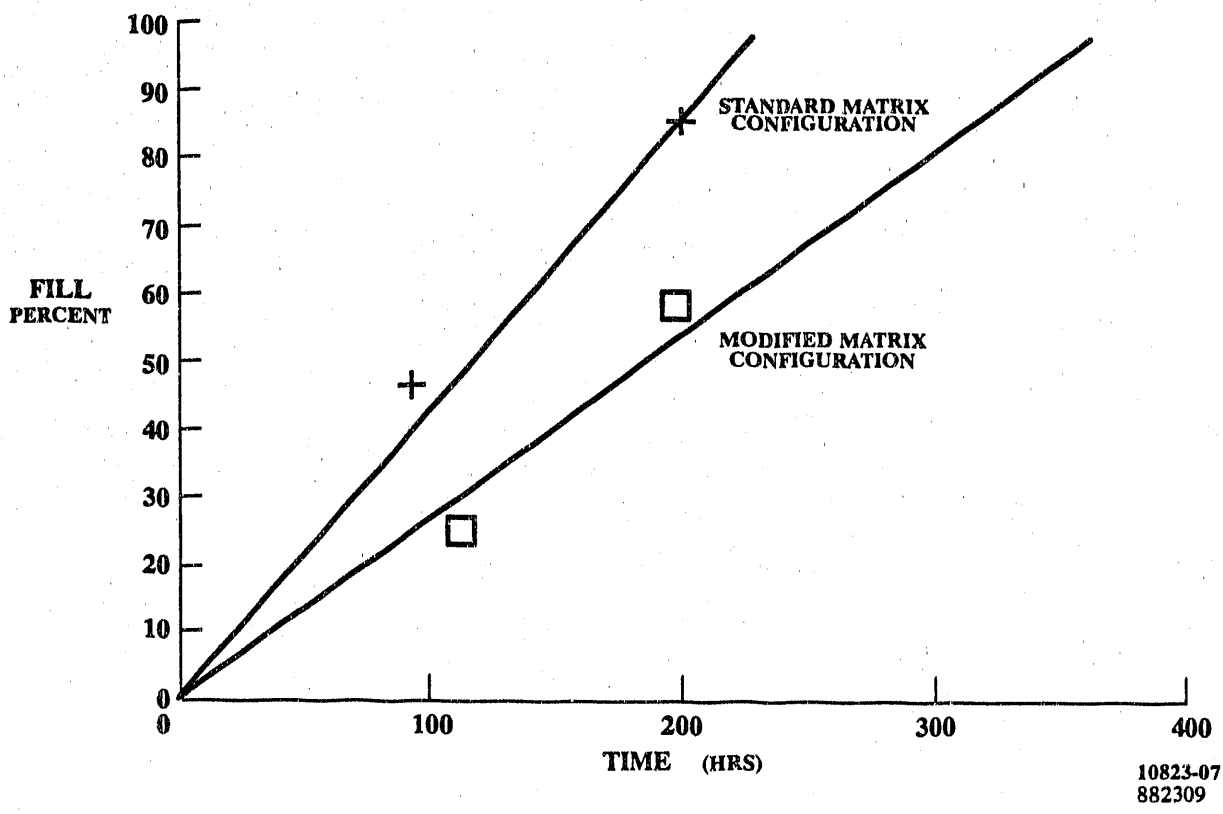

Figure 1.4-4. Percent Seal Fill vs. Time

SUBTASK 1.5 - DEVELOPMENT OF ANODE-SIDE COMPONENTS

Objective

Develop anode-side components that increase cell performance by reducing gas phase diffusional resistance, while providing 40,000 hour endurance for electrolyte storage in interior cells.

Process Development

Manufacturing processes were developed for the two anode-side components: the anode, which performs the hydrogen oxidation function, and the cell component which provides the function of electrolyte storage and the gas flow field. Requirements for these cell components were established in Subtask 1.3.

Trials were conducted to determine whether the preliminary geometry and porosity specifications for the anode could be achieved. The preliminary specifications suggested that this component could be fabricated by a tape casting process. A series of tape casting trials was conducted. Tapes cast from the first slurry were processed through burn out and sintering. These parts had acceptable geometry, but were below the porosity specification. Additional tape casting trials were then conducted using an alternative binder for the slurries. Slurries of several different recipes were made with the objective of increasing porosity to meet the design specification. Tapes were cast from each slurry and processed through sintering. The results of these trials were parts which met the design specifications for porosity, pore size distribution, and thickness. These parts were tested in Cell Nos. 632, 638, 642, and 649.

Anodes with a smaller median pore size and broader pore size distribution to meet the revised specification defined in Subtask 1.3 were then fabricated. The approach was to introduce an additive to the raw materials comprising the slurry for tape casting. Anodes were tape cast and heat treated. Mercury intrusion porosimetry showed that a smaller median pore size and a broader pore size distribution were achieved. Anodes of this type were tested in Cell Nos. 653 and 664.

Trials were conducted to form an anode gas diffusion layer from large particle size nickel by tape casting. Diffusion layers with acceptable porosity and median pore size were fabricated, but their sintered strength was not adequate. The only method by which a diffusion layer with adequate strength could be fabricated was as a bilayer in conjunction with the anode structure. This approach was considered too costly and the effort to develop a diffusion layer was discontinued. As reported in Subtask 1.3, the current collector design was modified to improve gas-phase diffusional characteristics.

Work was conducted to automate the tape casting process. An apparatus capable of casting subscale tapes was constructed and used to make several visually acceptable anode tapes. This equipment is intended to improve quality as well as provide data useful in scaling up the process to fabricate large area components.

Several runs were conducted to determine the effect of various process parameters on tape properties. The results of these trials were encouraging, and indicated that the automated casting process is a feasible method for producing anode electrode tapes.

Activity to tape cast large area anodes is reported under Subtask 2.2, Stack Repeat Component Fabrication.

Trials were conducted to determine the feasibility of fabricating the electrolyte storage and gas flow field component for anode-side Configuration C. Initial results indicate the configuration was feasible to fabricate. This configuration utilizes a combination of raw materials to achieve properties that permit sufficient electrolyte storage without significantly impeding diffusion of hydrogen to the oxidation sites. Fabrication trials indicated the combination of raw materials could be combined to produce the required part geometry. Fabrication focused on achieving the dimensional and pore size requirements of the design specification. Initial trials resulted in dimensional characteristics that closely match the specification, however, the pore size was larger than desired. The pore size was reduced by a raw material modification, but was still slightly larger than specification. The pore size was decreased by reducing the porosity relative to the previous trials. This component was tested in Cell No. 638.

Single Cell Testing of Anode-Side Components

Six cells were tested to evaluate new anode-side configurations. Cell No. 632 contained Configuration B components and Cell No. 638 contained Configuration C components. Cell Nos. 642, 649 and 653 contained Configuration D anode-side components. Cell No. 664 contained modified Configuration D anode-side components. All of these cells had standard cathode-side components. The performance of these cells is shown in Table 1.

The performances of Cell Nos. 632 and 638 at 1 atm. and 100 ASF were below that of the best performing cell (No. 633) using standard anode-side components (0.800 volts and 0.802 volts, respectively, compared to 0.831 volts for Cell No. 633). The results of diagnostic tests on these cells showed that the Configuration B anode-side configuration in Cell No. 632 performs at least equivalent to the best standard anode (Cell No. 634) tested in this program.

The performance of Cell No. 638 with Configuration C components showed steady decay during 800 hours of operation. The decay was attributed to the anode configuration.

Testing of Cell No. 632 was terminated after about 3500 hours of operation at atmospheric pressure. The performance history of this cell is shown in Figure 1.5-1. In the first 1000 hours, the performance of this cell declined by about 20 mV at 160 ASF. The performance was then constant for over 2000 hours until a slight increase in internal resistance caused a slight performance decline. Diagnostic tests showed the anode performed very well.

Both Cell Nos. 642 and 649 tested Configuration D components. Cell No. 642 was started with the cell inadvertently short circuited. Although cell performance increased to the range of normally started cells after the short circuit was removed, the data are considered suspect and the test was repeated in Cell No. 649. The performance levels were nevertheless similar for both of these cells as can be seen from Table 1. Diagnostic data also indicate similar anode performance losses which are in the range measured for standard anodes.

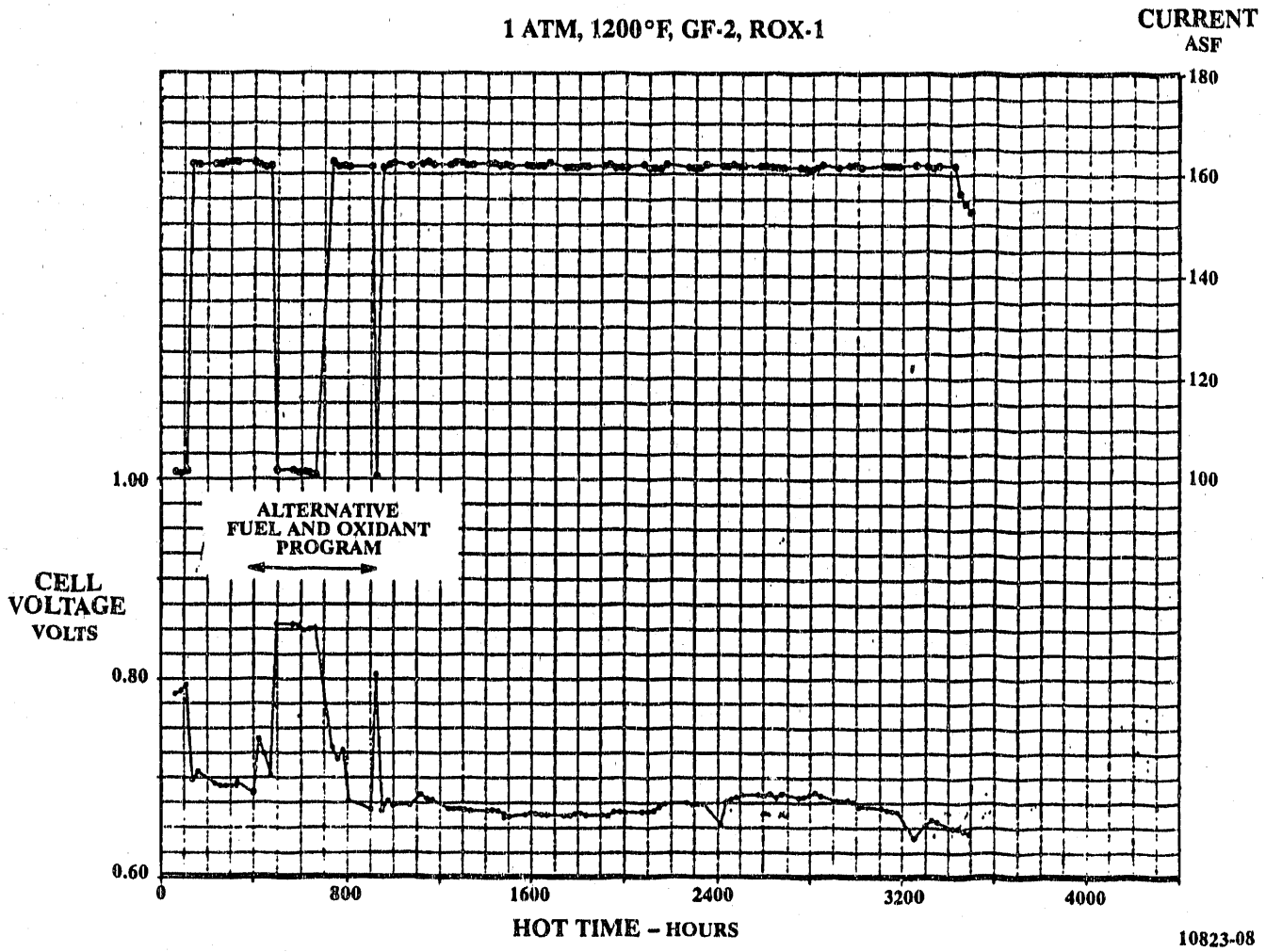

Figure 1.5-1. Performance History of Cell No. 632

Testing was performed on Cell No. 649 to determine the effect of thermal cycles on cell performance as a baseline for planned matrix evaluations. This testing was successfully completed and the cell was shut down with over 2000 hours test time.

Cell No. 653 is also Configuration D but the anode has a broader pore spectrum. This change provides a better matching of the anode and cathode pore spectra. The performance of Cell No. 653 was 0.800 volts at 100 ASF, a level near that of Cell Nos. 642 and 649. To obtain a direct measurement of individual electrode polarizations, Cell No. 653 was constructed with a reference electrode. Figure 1.5-2 shows the iR-free anode and cathode polarizations relative to the reference probe as a function of current density taken at constant flow conditions. The anode utilization at 250 ASF was 28.5 percent and the cathode utilization at 250 ASF was 12.5 percent. These low utilization data show that the anode polarization is 58 mV at 250 ASF indicating that the anode is performing well. This reference probe data is used to verify the diagnostic reduction routines used in the absence of a reference electrode.

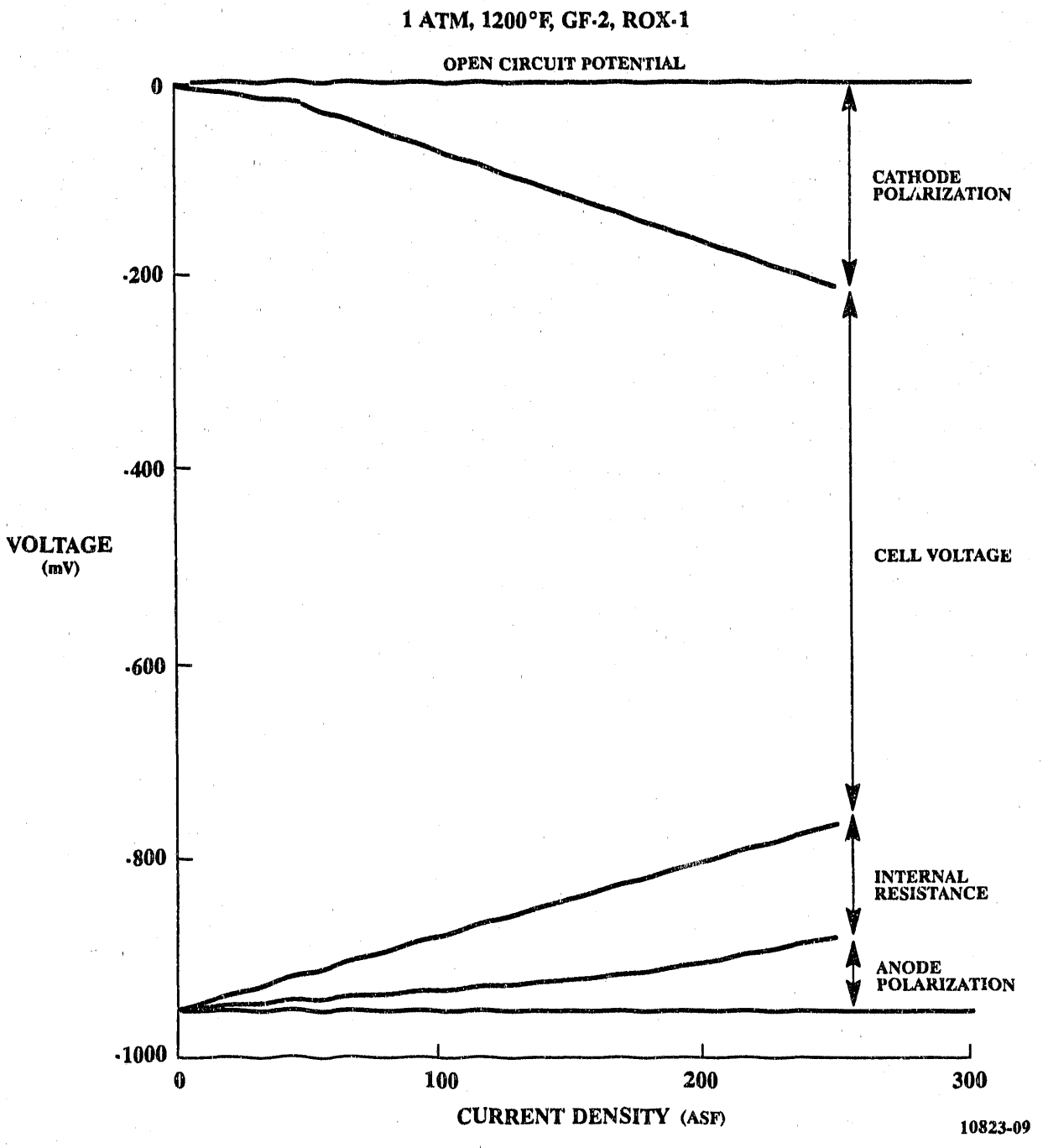

Figure 1.5-2. Anode and Cathode Polarizations (Cell No. 653)

Cell No. 664 contained modified Configuration D anode-side components designed to optimize gas diffusion. Cell No. 664 was tested to 2000 hours. The peak performance (0.828 volts at 100 ASF, 1 ATM) was very good and diagnostic testing showed good anode performance.

SUBTASK 1.6 - DEVELOPMENT OF CATHODE-SIDE COMPONENTS

Objective

Develop cathode-side components that reduce cathode compaction and reduce NiO dissolution rates. Determine and quantify the improvement in performance of the cathode resulting from higher CO_2 pressures.

Process Development

Process development work in this task focused on developing a tape casting process to fabricate cathodes to the specifications generated in Subtask 1.3.

Cathodes that were fabricated by a dry powder process were used in single cell tests while tape cast cathodes were being developed. These cathodes although not fabricated by the scalable tape casting process, did meet the preliminary design specifications for porosity, pore size distribution, and were near the dimensional requirements. These cathodes were tested in Cell Nos. 629, 634, 635, 648, 651, and 652.

Several approaches were evaluated in developing a tape casting process to meet the higher porosity requirement of the cathode and the revised pore size specification defined in Subtask 1.3 These include:

- Pore formers
- Blowing agents
- Restrict shrinkage during sintering
- Alternative binders

The approach that initially appeared to be the most successful in achieving the high porosity and revised pore size specification was to incorporate pore formers into the cathode tape. Mercury intrusion porosimetry indicated that the median pore diameter of a cathode fabricated with pore formers was larger and the pore size distribution was broader than a standard cathode at equivalent porosity. A cathode of this type was tested in Cell No. 643.

Problems with agglomeration of the pore formers was encountered in scaling up the slurry batch size for tape casting. Subsequently, an alternative binder system was identified for cathode tapes that produced sintered cathodes that met the porosity and revised pore size specification. Cathodes of this type were tested in Cell No. 660 and in Integrated Cells in Subtask 1.8.

Automated tape casting trials were conducted using the bench scale apparatus used for the anode trials in Subtask 1.5. The results of the trials indicate the process is suitable for producing cathode electrode tapes.

Work related to tape casting large area cathodes is reported under Subtask 2.2, Stack Repeat Component Fabrication.

Single Cell Testing

Ten cells were tested to evaluate cathode-side configurations. The performance of these cells is shown in Table 1. All of these cells had standard anode-side components.

Two cathode-side Configuration A cells, No. 629 and No. 634, differed only in electrolyte content, with No. 634 containing the lesser amount. Both of these cells showed significantly higher cathode performance losses than a standard cell based on diagnostic tests.

Cell Nos. 635, 641, 643, 648, 651, and 660 contained Configuration C cathode-side components.

Diagnostic tests showed Cell Nos. 635 and 641 had lower cathode performance losses compared to the Configuration A cells above. Cell No. 635 had lower cathode performance losses than the best standard cathode tested at this point in the program (Cell No. 630). Cell No. 641 had higher cathode performance losses than Cell No. 630, indicating a degree of irreproducibility.

Cell No. 643 was a Configuration C cell that contained a cathode with a larger median pore size and broader pore spectrum. This cell had a much lower performance, 0.737 volts at 100 ASF and 1 ATM, with an internal resistance loss of 59 mV. Diagnostics indicate that the cathode of this cell was probably flooded.

Cell No. 648 was a Configuration C cell tested to evaluate an intermediate thickness cathode. The peak iR-free performance was 855 mV at 100 ASF. The open circuit was low (.937 volts) due to a large crossover and large fuel and oxidant leakages from the cell. The cell was shut down for reasons other than the cathode.

Cell No. 651 was also a Configuration C cell with an intermediate thickness cathode. The peak iR-free performance was 862 mV at 100 ASF. Diagnostic tests show good cathode performance. Peak performance of 0.812 volts at 100 ASF, 1 ATM was reached.

Cell No. 660 contained Configuration C cathode-side components and was tested to measure cell compaction vs time. Three dial indicator gages were located around the periphery of the cell to determine cell movement. Total measured cell compaction at operating conditions was about 4 mils with most of the compaction occurring in the first 120 hours as shown in Figure 1.6-1. Post-test measurements confirmed this value. Upon disassembly it was found that the cell package did not fully seat, therefore, the actual load on the cell is uncertain. The cell performance was low (0.750 volts at 100 ASF, 1 ATM) and this is attributed to the cell not being fully seated.

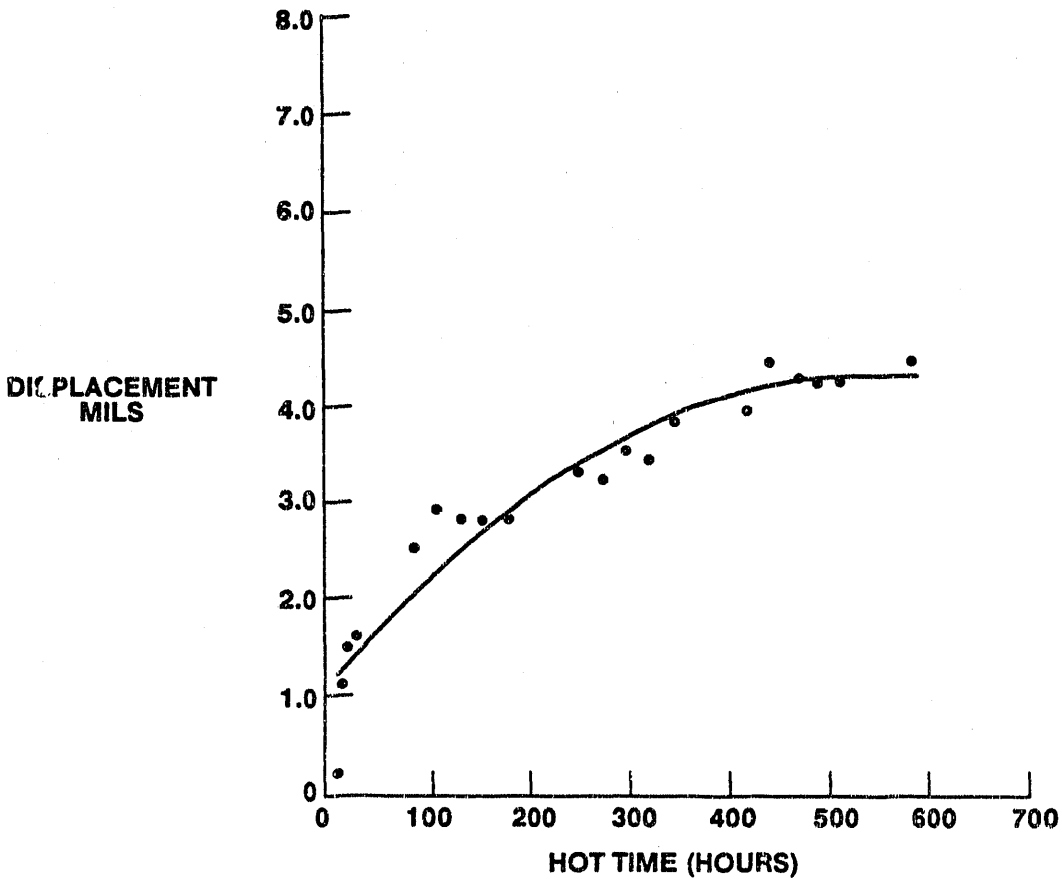

10823-10

Figure 1.6-1. Cell No. 660 Compaction Versus Time

Cell No. 652 was a modified Configuration B cathode configuration with components designed to minimize gas diffusion losses. The peak performance of this cell was very good (0.824 volts at 100 ASF, 1 ATM). Diagnostic tests showed excellent cathode performance with low gas phase diffusion losses. Additional testing was conducted using an oxidant lower in carbon dioxide content (7.2% vs. 18.1%). The resulting polarization increase was less than that for a standard cathode-side configuration. A modified Configuration B cathode-side configuration was designated as Configuration D and tested in most of the Integrated Cells in Subtask 1.8.

Cell No. 654 was tested to evaluate an alternative cathode structure. Initial diagnostics indicated that the cathode was flooded. Peak performance of 678 mV at 100 ASF and 1 ATM was obtained just prior to shutdown. The peak performance of this cell was very low and no further work was conducted on this cathode structure.

SUBTASK 1.7 - DEVELOPMENT OF END-CELL RESERVOIRS

Objective

Develop an electrolyte reservoir for end-cells which extends the projected life of stacks to 40,000 hours by providing additional reservoir capacity in those cells that experience a considerable change in electrolyte inventory due to migration from the positive to the negative end of the stack. The performance penalty of a cell operating with this increased reservoir capacity should not exceed 50 mV/250 ASF throughout its projected life.

Process Development

Three end-cell reservoir designs were defined. One of the designs utilizes a non-conductive electrolyte reservoir material and two designs utilize a conductive material.

Fabrication trials were conducted to produce the non-conductive electrolyte reservoir material that is specified for one of the three end-cell reservoir designs defined in Subtask 1.3. The trials resulted in an electrolyte reservoir material which had the required porosity and median pore size.

Two single cell tests were conducted to evaluate an end-cell reservoir design that utilizes the non-conductive electrolyte reservoir material. These were Cell No. 666 (fifth integrated cell) and Cell No. 674 (eighth integrated cell).

Cell No. 666 had low performance and a very high internal resistance. Teardown inspection showed the high iR to be caused by a contact problem with the end-cell reservoir.

Cell No. 674 had lower iR as a result of a modification to the reservoir design, but had very low performance due to flooded electrodes. The electrode flooding was attributed to the end-cell reservoir design. These two cells are reported in more detail in Subtask 1.8, Integrated Cell Testing.

Cell Nos. 666 and 674 showed the design with a non-conductive reservoir material to be unacceptable. No further work was conducted with the end-cell reservoir design that utilizes the non-conductive electrolyte reservoir material.

The second end-cell reservoir design evaluated was the first of two designs that utilize a conductive reservoir material. The conductive reservoir component was fabricated and tested in Cell No. 677. The performance of Cell No. 677 was very low at 0.700 volts at 100 ASF, 1 ATM, with an iR of 66 mV. The end-cell reservoir in this cell caused high anode polarization and was not considered to be an acceptable design.

The other end-cell reservoir design that utilizes a conductive material was then evaluated. Components for the second design with a conductive reservoir material were fabricated and included in Cell Nos. 695 and 699. The performance of these cells was good verifying the design of the conductive reservoir. These cells were tested under Subtask 4.1, but are included in this report for completeness.

SUBTASK 1.8 - SINGLE CELL TESTING OF IMPROVED ANODE AND CATHODE COMPONENTS INTEGRATED INTO ONE CELL

Objective

The objective is to combine the cell components being improved individually under Subtasks 1.4 through 1.6 into integrated benchscale cells, and test and analyze these cells in order to compare their data for compliance to the design objectives established for interior cells in Subtask 1.3.

Test Stations and Cell Hardware

Test stations for single cell testing in Subtasks 1.4 – 1.8 were prepared. Functional checks of the various systems and support equipment that serve the 16 ambient and 8 pressurized test stations were conducted. This included the temperature control system, reactant flow and control measurement system, humidification system, gas mix stations, and safety related equipment.

Five sets of cell hardware from the previous program were refurbished and 25 sets of new hardware were fabricated for single cell testing in Subtasks 1.4 – 1.8.

A standard cell (No. 624) which contained components fabricated in the previous program for the 8-ft^2 short stack was tested to check out the ambient test stand.

Cell No. 625 was tested to check out the pressurized test stand. This cell also served as a control for matrix shorting tests in Subtask 1.4.

Reference Electrode

Cell No. 626 was tested to evaluate a reference electrode on the cathode-side to provide a direct measurement of anode and cathode polarizations. The reference electrode did not provide valid diagnostic data and the cell test was terminated.

Diagnostic data from Cell No. 626 showed an incorrect split of cell polarization between the anode and cathode. This result appeared to be caused by the relatively large diameter of the reference electrode compared to the matrix thickness. The region of the anode opposite the reference electrode was probably operating near open circuit voltage with an in-plane potential gradient in the electrolyte under the reference electrode. The design of the reference electrode was modified to correct these deficiencies and was evaluated in another cell test (No. 630). Results indicated that the modified reference electrode was providing the desired cell diagnostic data.

The polarization measurements from the reference electrode in Cell No. 630 are shown in Figure 1.8-1. Reference electrodes were then used in selected cells throughout the program.

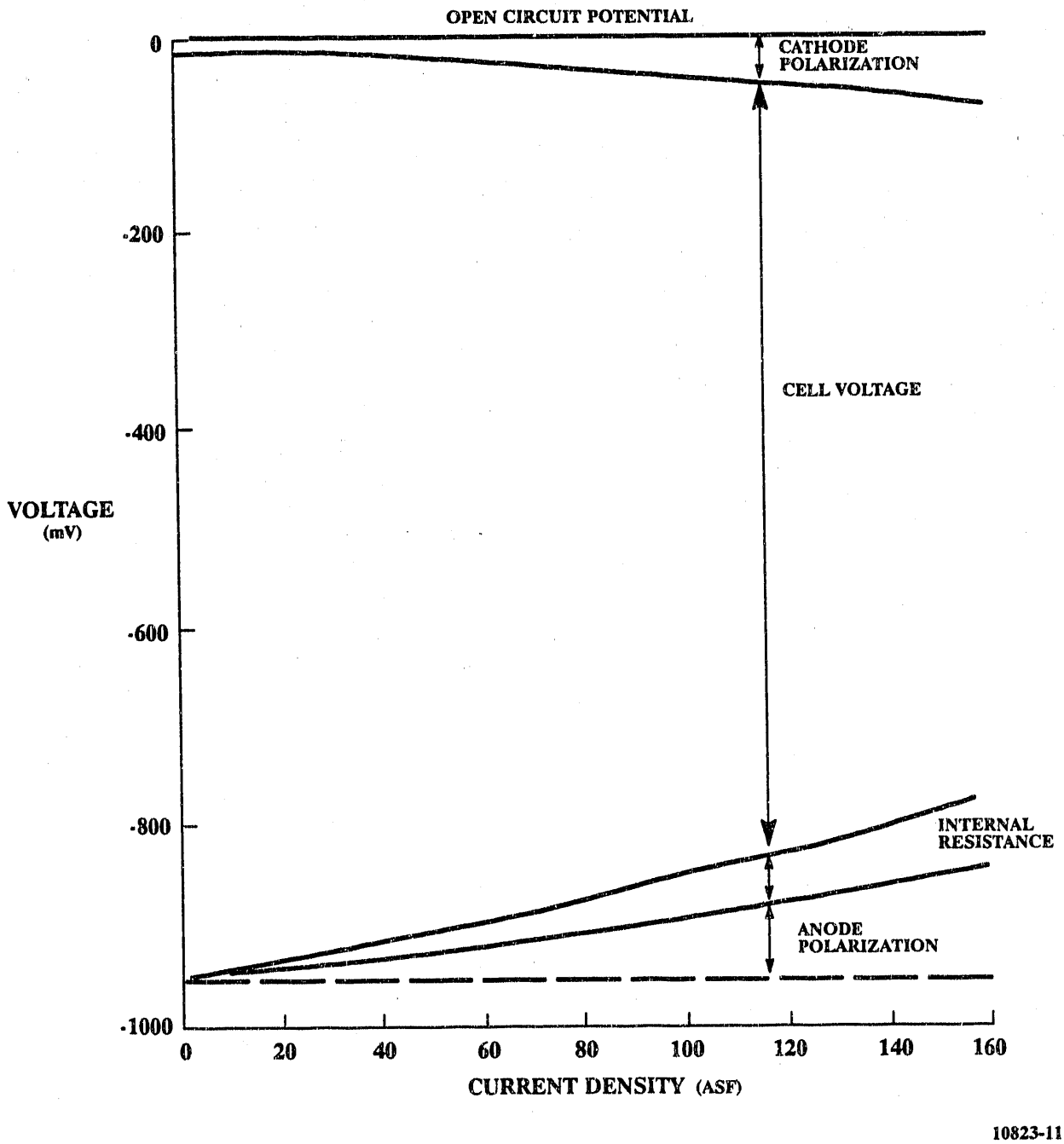

Figure 1.8-1. Anode and Cathode Polarizations (Cell No. 630)

Integrated Cell Testing

The first integrated cell (No. 639) incorporating new anode-and cathode-side components was tested for 850 hours. This cell contained Configuration D anode-side components and Configuration C cathode-side components. The initial performance of this cell was low and the internal resistance was high. The performance increased with time as shown in Figure 1.8-2. The slowly increasing performance and low peak performance are primarily attributed to improper electrolyte fill and initial distribution.

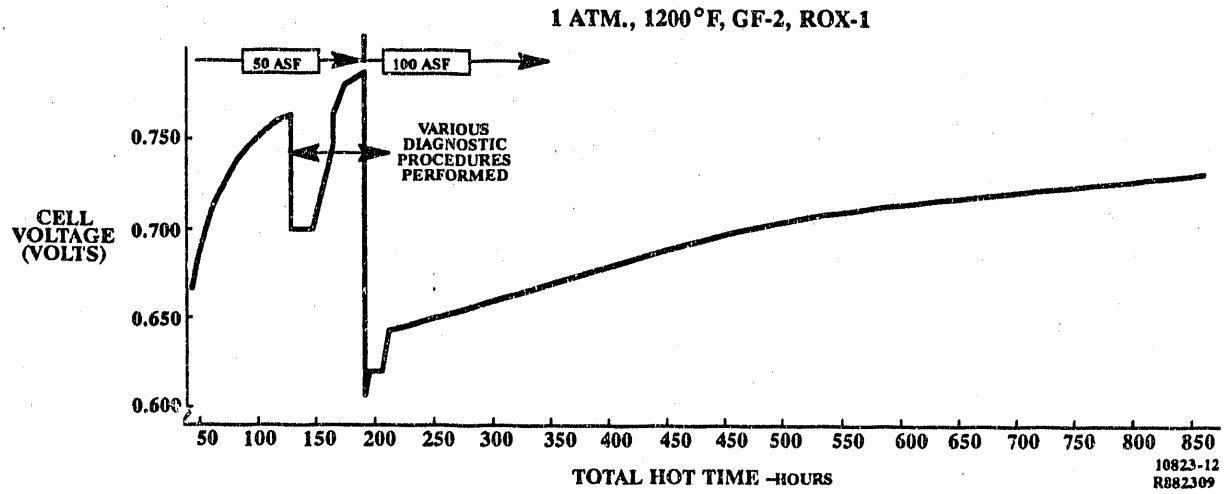

Figure 1.8-2. Performance History of Cell No. 639

The second integrated cell (No. 647) contained Configuration D anode-side components and Configuration C cathode-side components. Figure 1.8-3 shows the performance of the cell as a function of time at 100 ASF. The peak performance was .814 V at 100 ASF and 1 ATM with an internal resistance loss of 37 mV, resulting in an iR-free performance of .855 V. This is significantly better than the first integrated cell (No. 639) and is comparable with the better cells in the program. The limited electrolyte reservoir capacity in the cell was the cause for its rapid decay.

The third integrated cell (No. 655) contained Configuration D anode-side components and Configuration D cathode-side components. Figure 1.8-4 shows the performance of this cell as a function of time at 100 ASF and 1 ATM. The performance decreased until additional electrolyte was added at 150 hours and a 100 mV improvement occurred in the next 100 hours. The peak performance was .782 V at 100 ASF and 1 ATM with an internal resistance loss of 49 mV, resulting in an iR-free performance of 0.831 V. The performance of this cell was adversely affected by low open circuit voltage (25 mV below theoretical) which was due to high gas crossover across the matrix. Teardown of the cell revealed that the matrix failure was associated with the electrolyte reservoir that was located in the anode-side housing.

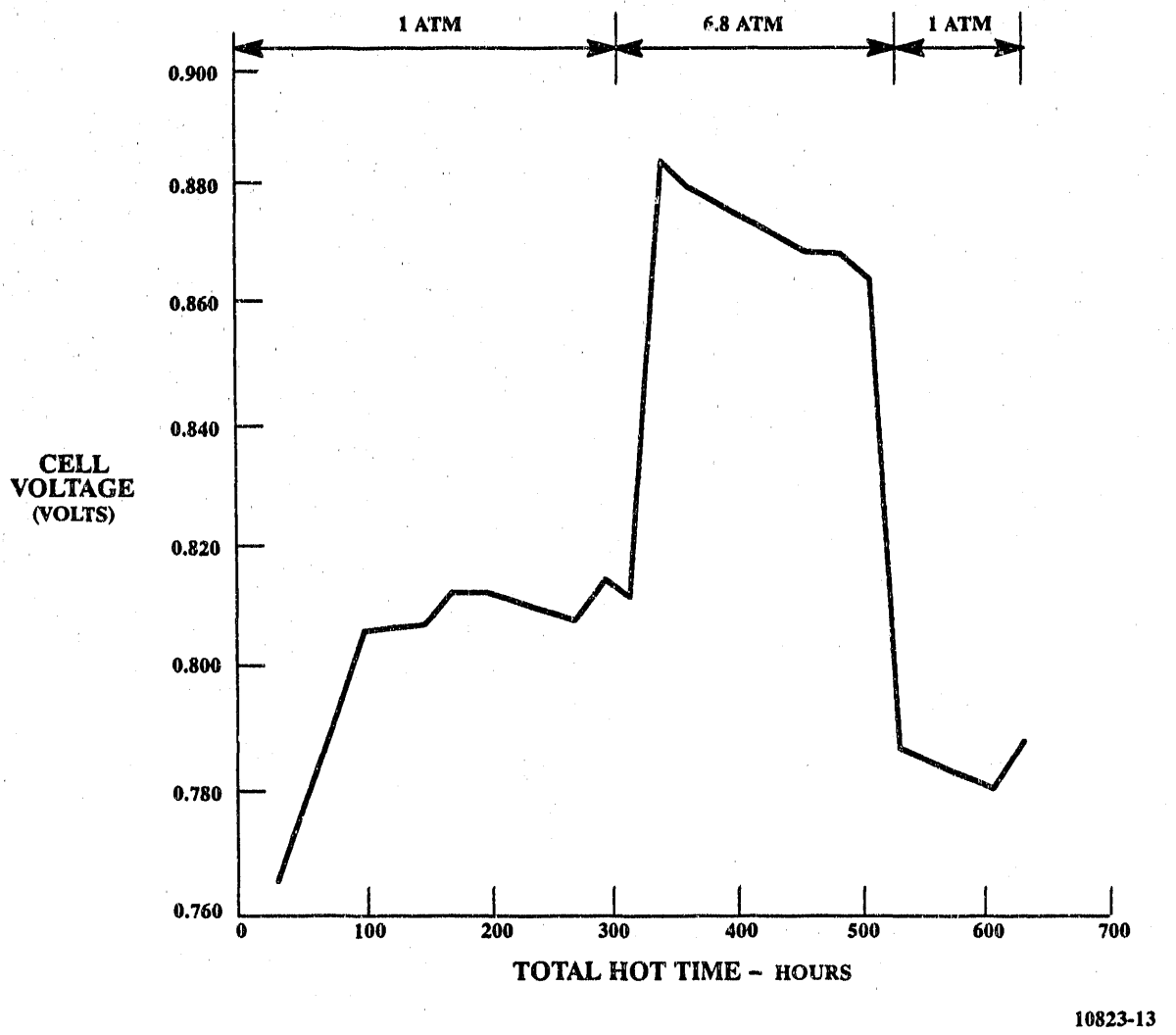

Figure 1.8-3. Performance History of Cell No. 647

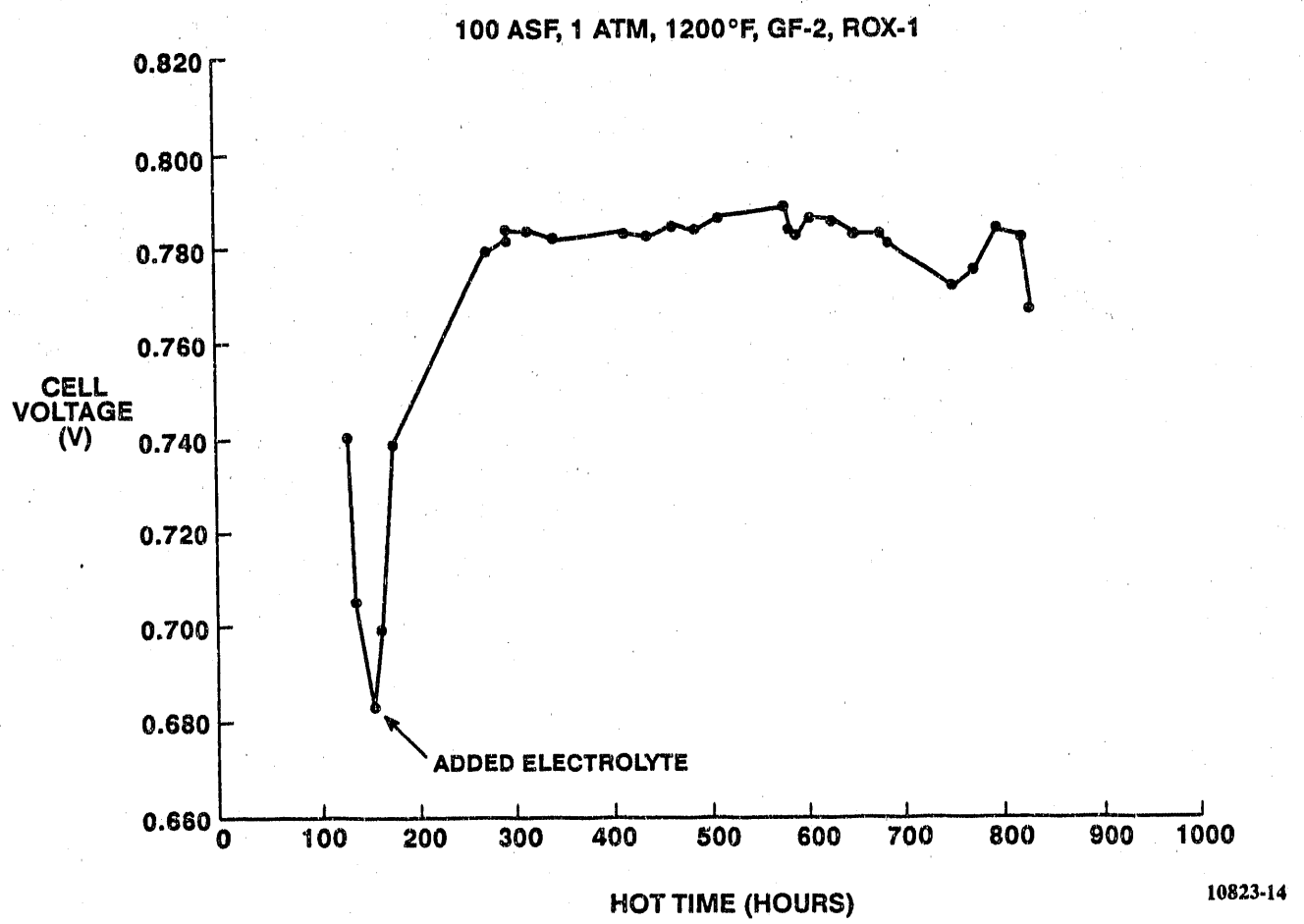

Figure 1.8-4. Performance History of Cell No. 655 (Third Integrated Cell)

The fourth integrated cell (No. 663) contained Configuration D anode-side components, Configuration D cathode-side components, and a reinforced matrix. The anode in this cell had a broader pore size distribution. The performance history at 100 ASF is shown in Figure 1.8-5. The iR-free performance was 883 mV near the end of the test which is as high as any cell tested to date. The high iR (75-80 mV at 100 ASF) is attributed to the absence of a protective coating on the anode current collector. Diagnostic testing showed both electrodes performed well.

The fifth integrated cell (No. 666) contained Configuration D anode-side components and Configuration D cathode-side components. The cell was also tested to evaluate an end-cell reservoir design which is described in Subtask 1.7. Cell performance was very poor (622 mV at 100 ASF, 1 ATM, with an iR of 185 mV). The testing was concluded at 185 hours, and upon disassembly the cause of the high iR was found to be a contact problem with the end-cell reservoir.

The sixth integrated cell (No. 671) contained Configuration D anode-side components and Configuration D cathode-side components. The early performance was 0.796 volts at 100 ASF, 1 ATM, with an iR of 52 mV. At 143 hours the cell experienced a sudden performance loss and when the test was concluded at 403 hours the iR was over 300 mV at 100 ASF. The sudden loss occurred during a holiday period without an operator in attendance. Teardown analysis showed the cell was extremely dry and crossover damaged the cathode.

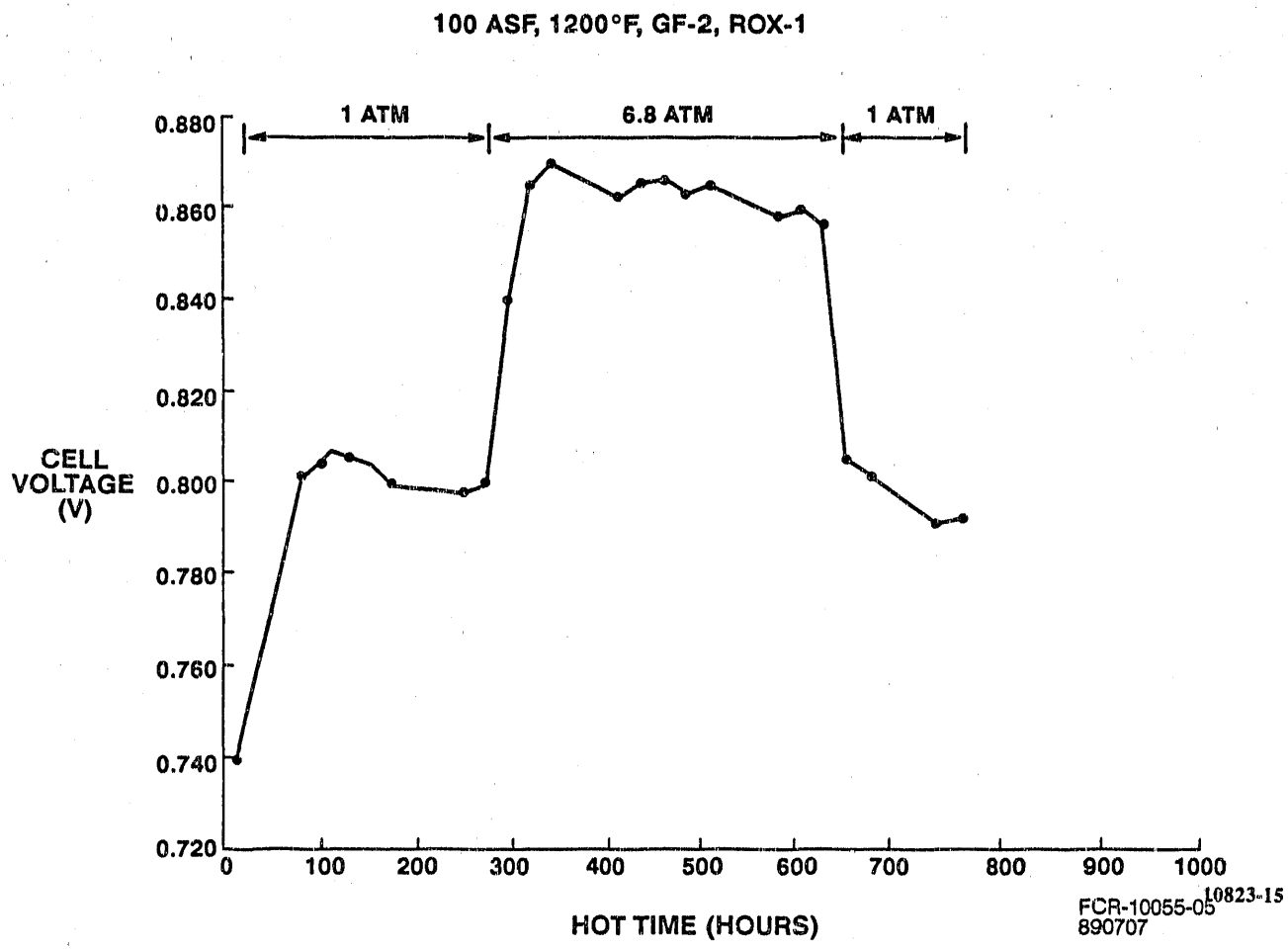

Figure 1.8-5. Performance History of Cell No. 663 (Fourth Integrated Cell)

The seventh integrated cell (No. 673) was essentially a repeat of the sixth. As seen in Table 1, the performance at 1 ATM and 6.8 ATM was superior to the best previous integrated cell (second, No. 647) even with the iR being higher by 5-10 mV/100 ASF. The performance history of Cell 673 is shown in Figure 1.8-6. This cell was also tested with oxidant and fuel compositions that are typical of a coal gasifier molten carbonate fuel cell system. The results of this testing are shown in Figures 1.8-7 and 1.8-8. There was no significant increase in cathode polarization at 250 ASF when the oxidant was changed from ROX-1 to the coal gasifier system lean oxidant composition (Figure 1.8-7). When the fuel was changed from GF-2 to the coal gasifier system lean fuel composition the anode polarization increased by about 45 mV at 250 ASF. (Figure 1.8-8).

The eight integrated cell (No. 674) was a repeat of the fifth integrated cell (No. 666). The end-cell reservoir was modified to eliminate the high iR experienced in Cell No. 666. In addition, the matrix was fabricated with the alternative materials discussed in Subtask 1.4. The improved cell iR (46 mV/100 ASF at the beginning of test) relative to Cell No. 666 indicated that the end-cell reservoir contact problem was solved. However, peak electrode performance was poor (698 mV at 100 ASF, 1 ATM with an iR of 63 mV) and cell behavior indicated that one or both electrodes were flooded. This was attributed to excessive electrolyte availability to the electrodes from the end-cell reservoir.

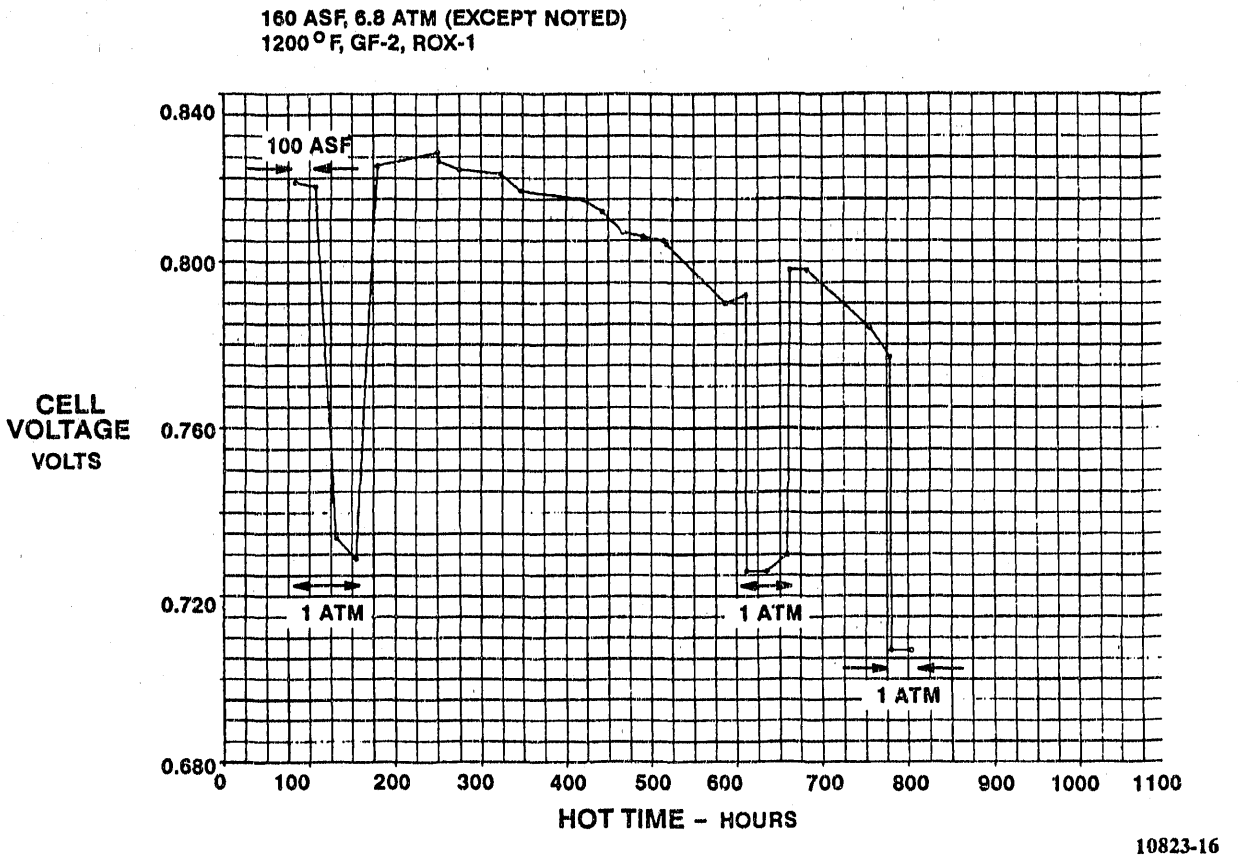

Figure 1.8-6. Performance History of Integrated Cell No. 673 (Seventh Integrated Cell)

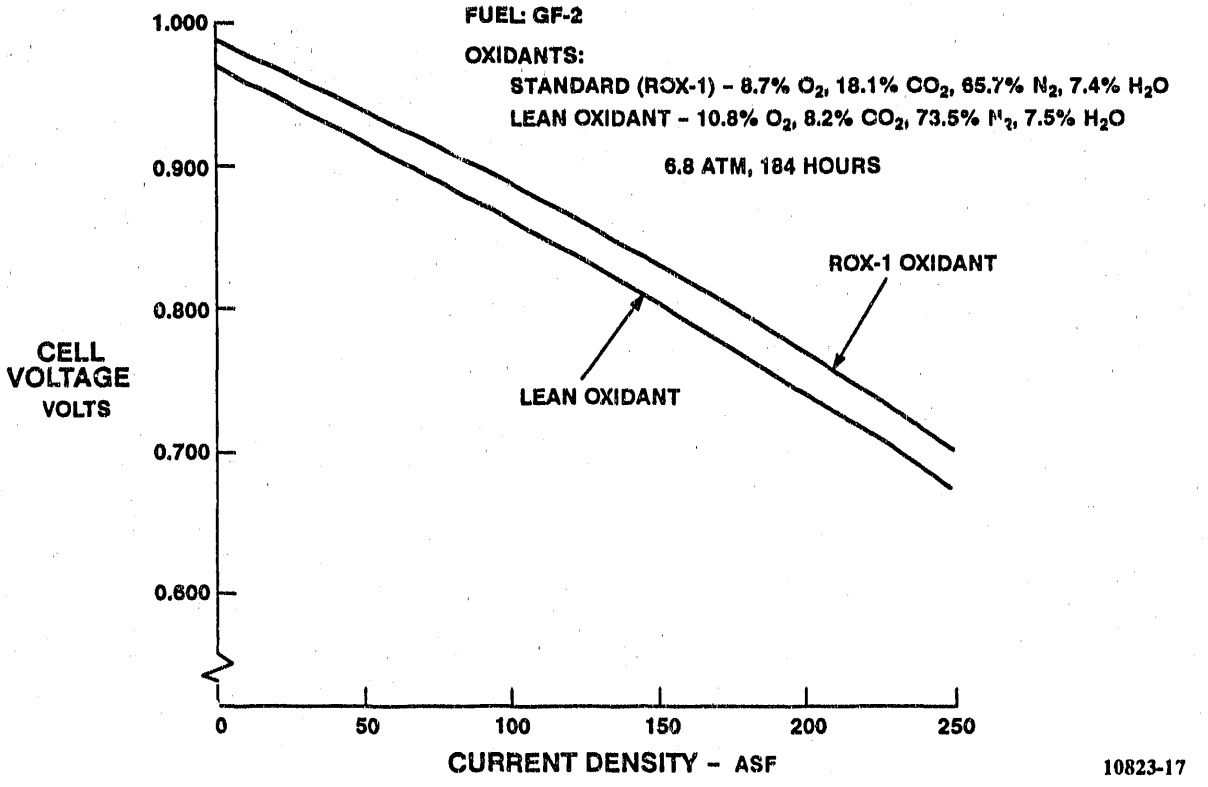

Figure 1.8-7. Performance of Cell No. 673 with Standard and Lean Oxidants

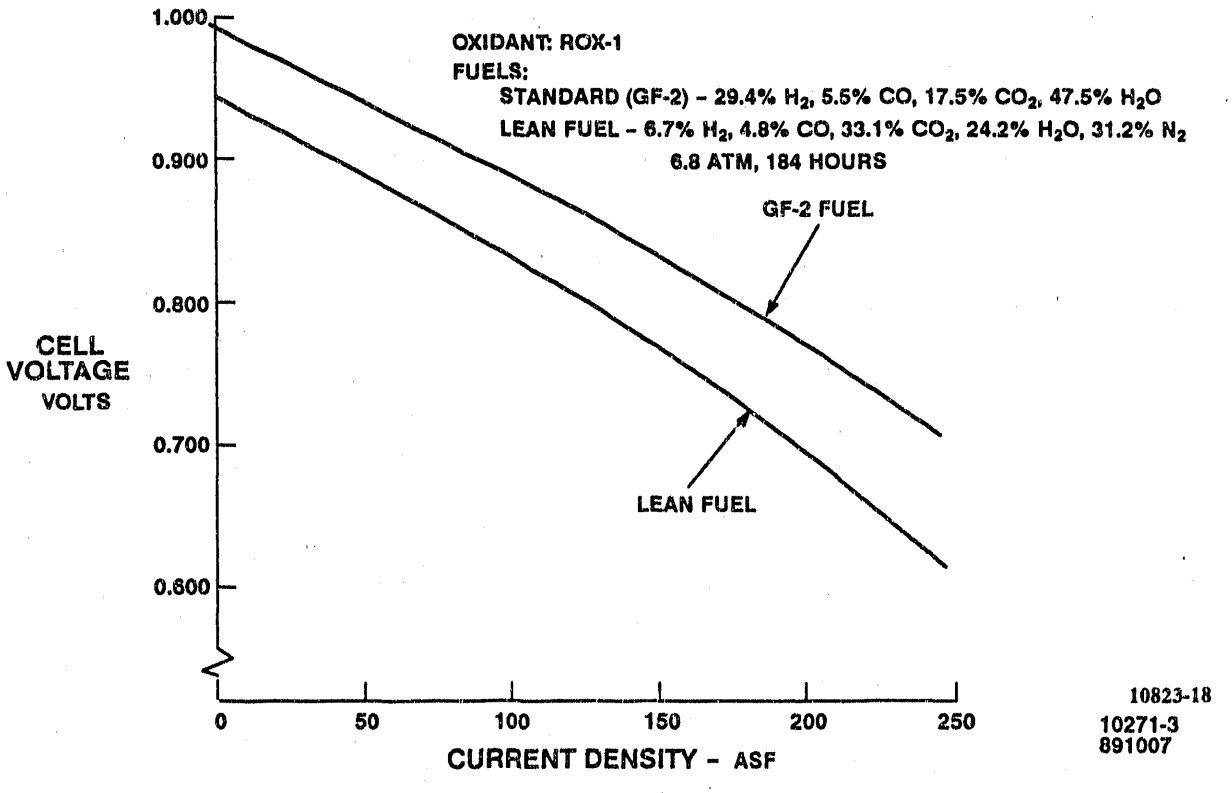

Figure 1.8-8. Performance of Cell No. 673 with Standard and Lean Fuels

The ninth integrated cell (No. 676) contained Configuration D anode-side components and Configuration D cathode-side components, and a matrix fabricated with the alternative materials. This cell was similar to the seventh integrated cell (No. 673) except for the electrolyte content and alternative matrix materials. The performance of this cell was initially low, but continued to increase throughout most of the 1900 hour test. Peak performance was 796 mV at 100 ASF, 1 ATM with an iR of 59 mV. The improving electrode performance confirmed the electrode flooding that was suspected early in the test. The performance history of cell No. 676 is shown in Figure 1.8-9.

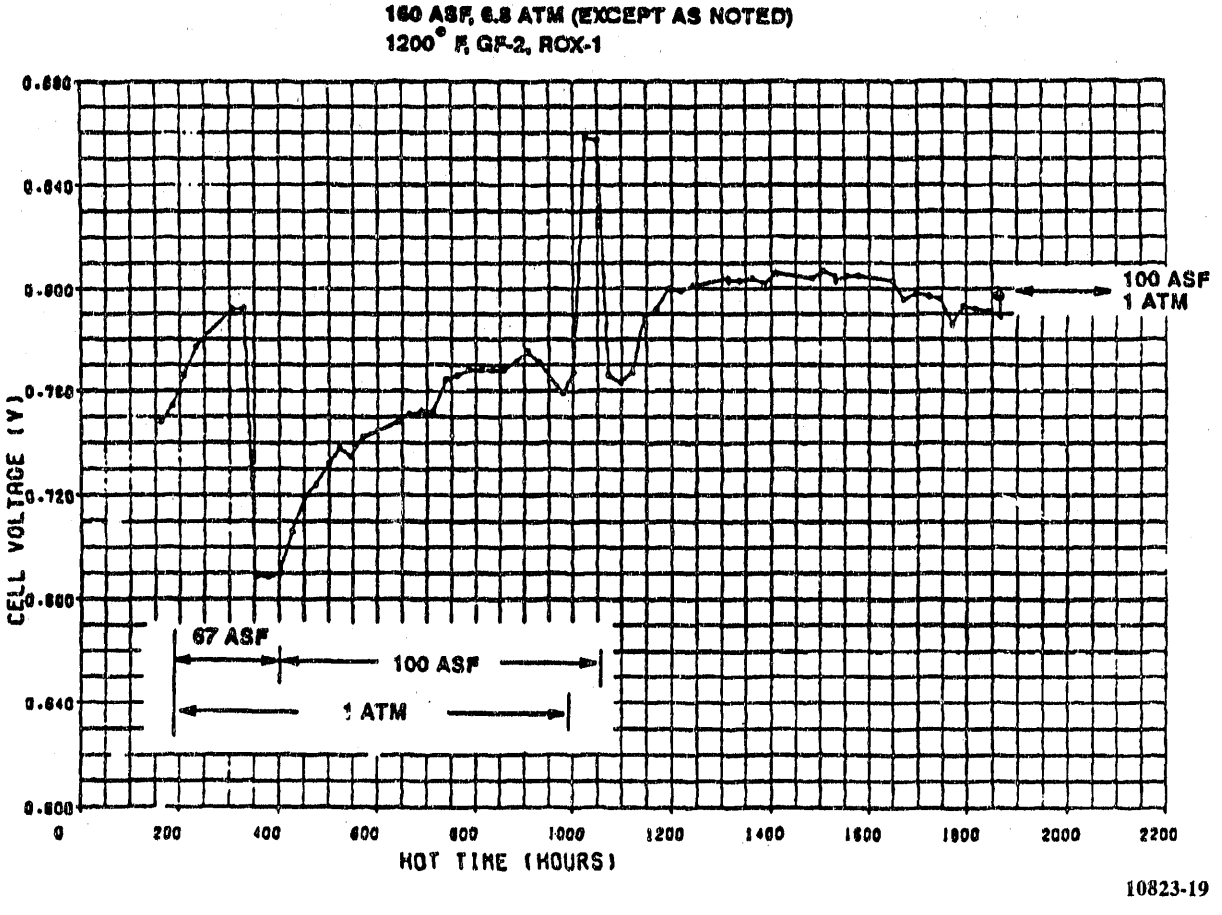

Figure 1.8-9. Performance History of Cell No. 676 (Ninth Integrated Cell)

The tenth integrated cell (No. 680) was similar to the ninth integrated cell (No. 676) but had a reduced electrolyte fill. The initial cell performance was poor and flooding was suspected. The cell was shut down early at 112 hours to determine the cause of flooding. The matrix was found to have more compaction than expected which would tend to flood the electrodes.

The eleventh and twelfth integrated cells (Nos. 689 and 690) were conducted to define the electrolyte fill and start-up procedures for the new cell configuration. These cells are reported in Subtask 4.1 along with additional cells tested to define the electrolyte fill and start-up procedures.

-END-

DATE FILMED

04 / 24 / 91